PRODUCTION OF THREE DIMENSIONAL POROUS SERS SUBSTRATES USING SILVER NANOPARTICLES-DECORATED EXPANDED GRAPHITE

Master of Science Thesis

Ayşe KURT
Eskişehir 2019

PRODUCTION OF THREE-DIMENSIONAL POROUS SERS SUBSTRATES USING SILVER NANOPARTICLE-DECORATED EXPANDED GRAPHITE

Ayşe KURT

MASTER OF SCIENCE THESIS

Department of Advanced Technologies
Programme in Nanotechnology
Supervisor: Assist. Prof. Dr. Yasemin ÇELİK

Eskişehir
Eskişehir Technical University
Institute of Graduate Programs
August 2019

FINAL APPROVAL FOR THESIS

This thesis titled "Production of Three-Dimensional Porous SERS Substrates Using Silver Nanoparticle-Decorated Expanded Graphite" has been prepared and submitted by Ayşe KURT in partial fulfilment of the requirements in "Eskişehir Technical University Directive on Graduate Education and Examination" for the Degree of Master of Science in Department of Advanced Technologies has been examined and approved on 09/08/2019.

Committee Members	**Title, Name and Surname**	**Signature**
Member (Supervisor)	: Assist. Prof. Dr. Yasemin ÇELİK	.....
Member	: Prof. Dr. Aydın DOĞAN	.....
Member	: Assist. Prof. Dr. Göktuğ GÜNKAYA	.....

Prof. Dr. Murat TANIŞLI
Director of Graduate School of Sciences

ABSTRACT

PRODUCTION OF THREE-DIMENSIONAL POROUS SERS SUBSTRATES USING SILVER NANOPARTICLE-DECORATED EXPANDED GRAPHITE

Ayşe KURT

Department of Advanced Technologies
Programme in Nanotechnology
Eskişehir Technical University, Institute of Graduate Programs, August 2019

Supervisor: Assist. Prof. Dr. Yasemin ÇELİK

Surface enhanced Raman spectroscopy (SERS) is a promising technique for single molecule detection, food safety, medical diagnostics and bio-sensing applications. However, relatively poor stability of the present substrates, high production costs due to need of sophisticated equipments, and repeatability problems limit the use of SERS as a routine analysis technique. Three dimensional (3D) porous platforms that contain metal nanostructures are highly promising for SERS applications due to fast penetration of solvent into the substrate and enabling to adsorb more metal nanoparticles and analyte molecules because of their high specific surface area. However, it is a prerequisite to develop these platforms with a low cost.

In this thesis study, 3D porous substrates were prepared from expanded graphite (EG) which was decorated by silver nanoparticles (AgNPs), and their SERS-activity was investigated. EG is a relatively low cost material with a highly porous structure, high specific surface area and reactivity, which allow adsorption of large amount of nanoparticles and analyte molecules. Accordingly, spherical AgNPs in the size range of 20-100 nm were successfully synthesized by chemical reduction of $AgNO_3$ in solution phase method and uniformly mixed with EG. The obtained EG/AgNPs nanocomposite powders were compacted in the form of a pellet and their SERS activity was tested using R6G dye. R6G solutions with different concentrations 10^{-3} – 10^{-12} M were dropped onto the substrates and the solvent penetrated into the substrate within a few minutes, enabling to perform SERS analyses immediately. The detection limit of EG for R6G was determined as 10^{-7} M, while the detection limit was lowered to 10^{-11} M when EG was decorated with AgNPs which were synthesized using ascorbic acid as a reducing agent.

Keywords: Surface enhanced Raman spectroscopy, SERS, Three-dimensional porous platforms, Silver nanoparticles, Expanded graphite.

ÖZET

GÜMÜŞ NANOPARTİKÜL İLE DEKORE EDİLEN GENİŞLETİLMİŞ GRAFİT İLE ÜÇ BOYUTLU GÖZENEKLİ SERS ÜRETİMİ

Ayşe KURT

İleri Teknolojiler Anabilim Dalı
Nanoteknoloji Bilim Dalı
Eskişehir Teknik Üniversitesi, Lisansüstü Eğitim Enstitüsü, Ağustos 2019

Danışman: Dr. Öğr. Üyesi Yasemin ÇELİK

Yüzeyde güçlendirilmiş Raman spektroskopisi (SERS) tek molekül algılama, analitik kimya, gıda güvenliği, tıbbi teşhis ve biyo-algılama gibi alanlarda oldukça yüksek potansiyele sahip olmasına rağmen, geliştirilen altlıkların yeterince kararlı olmaması, maliyetlerinin yüksek olması ve tekrarlanabilir ölçümler alınmasında karşılaşılan güçlükler nedeniyle rutin analizler için kullanılamamaktadır. Metal nanoyapıları içeren üç boyutlu (3D) gözenekli platformlar yüksek spesifik yüzey alanları nedeniyle çözücünün altlığa hızlı bir şekilde nüfuz etmesini ve daha fazla metal nanopartikül/analit molekülü adsorbe edilmesini sağladığından SERS uygulamaları için oldukça umut vericidir.

Bu tez çalışmasında, 3D gözenekli substratlar, genişletilmiş grafitin (EG) gümüş nanopartikül (AgNP) ile dekore edilmesiyle hazırlandı ve SERS aktiviteleri araştırıldı. EG, yüksek miktarda gözenekli yapıya, yüksek spesifik yüzey alanına ve reaktiviteye sahip olduğundan çok miktarda metal nanopartikülün ve analit molekülünün yüzeyine kolayca tutunmasını sağlayan oldukça düşük maliyetli bir malzemedir. 20-100 nm boyutundaki küresel AgNP'ler, $AgN0_3$'ün çözelti fazında kimyasal indirgenmesi ile başarılı bir şekilde sentezlendi ve EG ile düzgün bir şekilde karıştırıldı. Sıkıştırılmış EG ve EG/AgNP nanokompozit tozlarının SERS aktivitesini belirlemek için R6G boyası kullanıldı. Farklı konsantrasyonlardaki R6G çözeltileri 10^{-3}-10^{-12} M, SERS analizlerini hemen yapabilmek için altlıklara damlatıldı. EG'nin R6G için tespit limiti 10^{-7} M olarak belirlenirken, EG indirgeyici ajan olarak askorbik asit kullanılarak sentezlenen AgNP'lerle dekore edildiğinde tespit limiti 10^{-11} M'ye düşürüldü.

Anahtar Sözcükler: Yüzeyde güçlendirilmiş Raman spektroskopisi, SERS, Üç boyutlu gözenekli platformlar, Gümüş nanopartikül, Genişletilmiş grafit.

To my late mother…

ACKNOWLEDGEMENTS

I would like to thank my supervisor Assist. Prof. Dr. Yasemin Çelik for her guidance, appreciation and sincere advice. Her endless encouragement has been a major driving force during my thesis.

I would like to thank SUVACI Research Group for their support and friendship.

I am also thankful to Özgü Çalın and my lab colleagues Hasan Hüseyin Hizmetçi and Özge Yıldız for their help and friendship.

I would like to thank my mother, my father, and my sister for their encouragements during my education period and for their endless love and support.

09/08/2019

STATEMENT OF COMPLIANCE WITH ETHICAL PRINCIPLES AND RULES

I hereby truthfully declare that this thesis is an original work prepared by me; that I have behaved in accordance with the scientific ethical principles and rules throughout the stages of preparation, data collection, analysis and presentation of my work; that I have cited the sources of all the data and information that could be obtained within the scope of this study, and included these sources in the references section; and that this study has been scanned for plagiarism with "scientific plagiarism detection program" used by Eskişehir Technical University, and that "it does not have any plagiarism" whatsoever. I also declare that, if a case contrary to my declaration is detected in my work at any time, I hereby express my consent to all the ethical and legal consequences that are involved.

Ayşe KURT

TABLE OF CONTENTS

Page

LIST OF TABLES

Page

LIST OF FIGURES

Page

LIST OF ABBREVIATIONS

2D	: Two dimensional
3D	: Three dimensional
AA	: Ascorbic acid
Ag^+	: Silver ion
Ag^0	: Zero-valence state of silver
$AgNO_3$	: Silver nitrate
AgNPs	: Silver nanoparticles
Au	: Gold
Cu	: Copper
CVD	: Chemical vapor deposition
EDX	: Energy-dispersive x-ray spectroscopy
EF	: Enhancement factor
EG-AgNPs_AA	: Expanded graphite substrates decorated with silver nanoparticles produced by ascorbic acid as a reducing agent
EG-AgNPs_HH	: Expanded graphite substrates decorated with silver nanoparticles produced by hdroxylamine hydrochloride as a reducing agent
EG	: Expanded graphite
FEG-SEM	: Field emission gun scanning electron microscope
FTIR	: Fourier-transform infrared spectroscopy
HH	: Hydroxylamine hydrochloride
IR	: Infrared

LSPR	: Localized surface plasmon resonances
$NaBH_4$	: Sodium borohydride
NIR	: Near-infrared spectroscopy
NMP	: N-Methylpyrrolidone
R6G	: Rhodamine 6G
SERS	: Surface enhanced Raman spectroscopy
SPR	: Surface plasmon resonance
TSC	: Trisodium citrate
XRD	: X-ray diffractometer

1. INTRODUCTION

SERS is a powerful technique for the detection of very low concentration of a wide range of organic molecules including explosives, biomolecules and environmental pollutants. To improve the detection sensitivity and minimize fluorescence interference, SERS includes nanostructures to increase Raman intensity of analytes and eliminate background fluorescence. Nanostructures especially metal nanoparticles with controlled sizes and shapes, supports Raman signals of analyte molecules.

Colloidal nanoparticles make SERS measurements easy and cost-effective because they are relatively easy to manufacture and do not require complex devices. The analyte molecules are easily captured by colloidal nanoparticles, allowing rapid analysis. Metals such as silver (Ag), gold (Au) and copper (Cu) are the most commonly used elements in SERS applications due to their high SERS signal increase. Au and Cu show inter-band absorption in the apparent wavelength range, while inter-band absorption in Ag occurs in the ultraviolet wavelength range. Therefore, the highest SERS increase for visible light among these metals is achieved with Ag. Moreover, Ag is one of the most preferred noble metals in SERS applications due to its high plasmonic strengthening effect, low optical frequency loss and low cost compared to other noble metals. However, the intensity of the SERS signal strongly depends on the aggregation state of the colloids. Moreover, the so-called “coffee-ring” effect, which arises from capillary flow during drying of nanoparticle/analyte drop on a platform, leads to a non-uniform distribution of nanoparticles/analyte molecules. Therefore, it is a prerequisite to develop SERS-active substrates which provide uniform distribution of metal nanoparticles and help to prevent coffee-ring effect with a low cost.

Three dimensional (3D) porous platforms are highly promising for SERS applications due to fast penetration of solvent into the substrate, which eliminates coffee-ring effect and enables one to perform fast Raman measurements, and the ability of adsorbing more metal nanoparticles and analyte molecules because of their high specific surface area. However, the 3D substrates proposed for SERS analysis generally require sophisticated equipments, which make them too costly for routine SERS measurements.

In this thesis, 3D-porous substrates composed of expanded graphite (EG) decorated with silver nanoparticles (AgNPs) were proposed as a high performance and low cost SERS platforms.

Accordingly, the research objectives of this thesis are:

i. To synthesize AgNPs with a controlled shape and size (spherical in shape, 20-100 nm in diameter,with as narrow particle size distribution as possible)

ii. To uniformly decorate EG with AgNPs using rotary evaporator and obtain EG/AgNPs nanocomposite powders.

iii. To successfully compact EG/AgNPs nanocomposites into 3D-porous substrates.

iv. To investigate the SERS performance of these 3D-porous EG/AgNPs substrates by using Rhodamine 6G as a testing analyte.

2. RAMAN SPECTROSCOPY

The energy of a molecule consists of discrete energy levels, which are partly composed of electronic, vibrational and rotational states [1]. When light interacts with matter, transition between these states is observed depending on the magnitude of energy used for excitation. If the molecule changes any of its energy states, light can be absorbed or scattered. Transition between vibrational or rotational energy levels in a molecule occur when light of higher frequencies interact with molecule. This process is called Raman scattering [2].

Raman scattering is a two-photon inelastic light scattering process. When incident photon of energy hv_0 (h = planck constant, v_0 = frequency) interact with matter, the energy of the molecule promotes from the ground state to a virtual state. This state is not real states and molecule relaxes by re-emitting photon immediately. If the scattered photon has the same frequency as the incident photon, this is called Rayleigh or elastic scattering. This type of scattering is the more intense form and its scattered intensity is 10^{-3} times less than that of the incident light which means that there is no change of energy between molecule and photon during the scattering process. However, a very small portion of incident light is alter to vibrational energy level of molecule ($hv_0 \pm hv_s$). There is an energy change resulting in energy loss or gain between the photon and the molecule during the scattering process. This type of scattering is called as Raman scattering. There are two types of Raman scattering. If the molecule absorbs an energy from the scattered photon, this is called Stokes Raman scattering ($hv_0 - hv_s$). Other one is called Anti-Stokes Raman scattering in which the energy is transferred from the molecule to the scattered photon ($hv_0 + hv_s$) [2-4]. These interactions are shown in Fig 2.1.

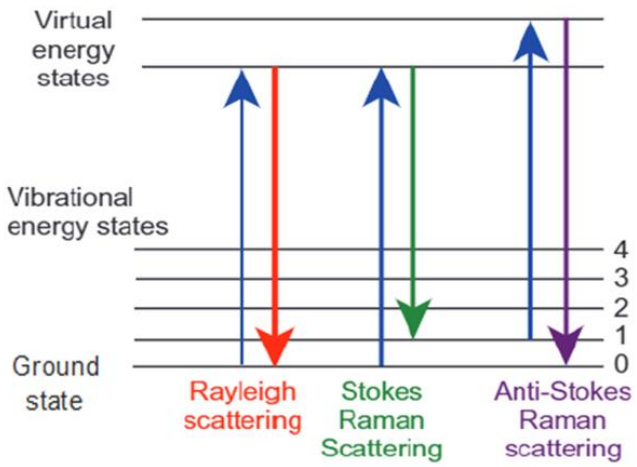

Figure 2.1. *Schematic illustration of Rayleigh and Raman scattering [5].*

Raman spectroscopy is a molecular spectroscopy technique used to determine molecular vibrations (phonon). The energy difference between the incident light and the Raman scattered light is called as a Raman shift. The Raman spectrum is basically plotting of intensity of scattered photon versus Raman shift. Since each type of molecule has its own vibration profile, bands in Raman spectrum represent characteristics of that molecule [5]. The height, width and position of the bands in the Raman spectrum can be measured to obtain information about the relative amount of material, layer thickness and degree of crystallinity [6]. It is a powerful analytical method for providing molecular fingerprint of samples and also for observing changes in molecular bond structure (for example, state changes, stresses and strains.) Moreover, different crystal structures of the same substance (polymorphs, allotropes) can be precisely distinguished via Raman spectroscopy [7].

Raman spectroscopy has great advantages over other vibrational techniques such as Fourier-transform infrared spectroscopy (FTIR) and Near-infrared spectroscopy (NIR). These advantages are that the Raman effect is released from the sample rather than the light absorbed by the sample. Therefore, Raman spectroscopy is not affected by water-related absorption bands and requires almost no sample preparation. This feature of Raman spectroscopy allows the characterization of gas, liquid and solid samples [8].

Raman and Infrared (IR) spectroscopies are complementary techniques. In order for a vibration to be IR active, there must be a change in dipole moment during the vibration of the

molecule, and for Raman to be active, it is necessary that the molecular vibration must result in a change in polarizability of the molecule. The most active bonds in IR spectroscopy are the covalent bonds with the highest dipole moment, while the most active bonds in Raman spectroscopy are those with the lowest dipole moment [1]. However, the Raman signals are inherently weak, so the number of inelastic scattered photons that can be used for analysis is very low. Raman signals can be significantly increased when a molecule adsorbed on or close proximity to nanostructured metal surfaces. This phenomenon is called surface enhanced Raman spectroscopy (SERS) [3].

3. SURFACE ENHANCED RAMAN SPECTROSCOPY (SERS)

3.1. Overview of SERS

SERS is a technique that extends the scope of Raman applications to include the detection of diluted and trace amounts of substances (for example, an impurity of one millionth in water) [9]. In Raman spectroscopy, only a very small portion of the incident photons (10^{-6}) are scattered. This makes Raman spectroscopy suitable for structural analysis rather than trace quantity analysis. On the other hand, SERS provides an enhanced Raman signal for analyte molecules that are adsorbed to the surface of nanoparticles/nanostructures or located around the gaps between nanoparticle arrays or aggregates called "hot-spots", or located at the ends or sharp edges of individual nanoparticles (Fig. 3.1) [11].

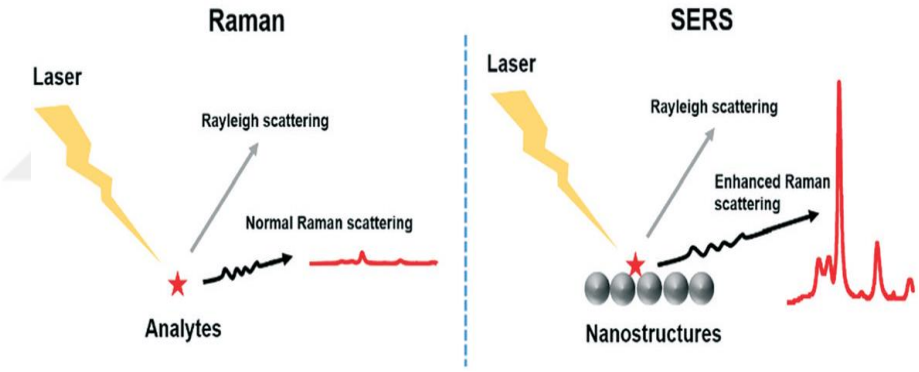

Figure 3.1. *Comparison between the Raman technique and the SERS technique [10].*

SERS technique is a promising analysis method for many areas such as analytical chemistry, food safety, biosensing, medical diagnostic and environmental monitoring due to its unique sensitivity and selective molecule detection properties. SERS allows to detect trace amounts of substances - in some cases up to a single molecule level - quickly, selectively and without damaging the analyte [9].

3.2. Historical Development of SERS Method

In 1974, Fleischmann *et al.* [12] found that roughened surface of Ag electrode produced strong SERS signals for molecule adsorbed to its surface and attributed this phenomenon to an increase in surface area [12,13]. The foundations of SERS theory and understanding were

laid in 1977 by Jeanmaire and Van Duyne [14] and Albrecht and Creighton [15]. In 1978, Moskovits [16] proposed that the large increase in Raman cross-section was the result of excitation of surface plasmons. This suggestion led to an idea that SERS could also be observed in metal colloids. Thus, there had been great a progress in the understanding developed on SERS. However, interest in SERS had decreased due to unrepeatability of the experiments, the specific nature of analyte, and relatively low signal increases. In 1997, two research groups, Nie and Emory [17] and Kneipp *et al.* [18], simultaneously and independently, reported that sufficiently intense SERS signals could be recorded for single-molecule detection under appropriate conditions. Thus, there has been a renewed interest in SERS with the detection of single molecules. SERS has been worked again as a research area for high-precision molecular detection platforms and many publications have been published in this field. The significant increase in the number of publications on SERS technique in recent years can be seen in Figure 3.2.

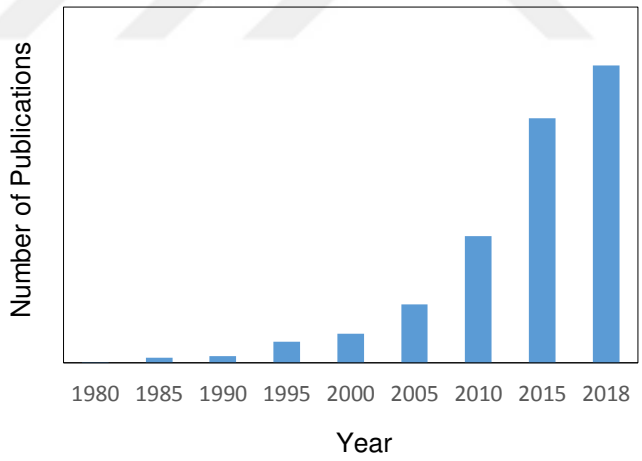

Figure 3.2. *Graphical representation of the number of publications on SERS by years identified by searching "surface enhanced Raman spectroscopy" in Web of Science (Web of Science accessed date: 07 April 2019).*

3.3. Mechanism of SERS

In SERS technique, the effective Raman scattering signal is significantly enhanced by bonding molecules onto the metallic nanostructures. Although the mechanism of enhancement of the Raman signal has not been fully understood, yet two mechanisms are thought to be effective. These are the "electromagnetic effect" resulting from the optical properties of the

nanostructured metallic surfaces and "chemical effect" resulting from the charge transfer between the metal surface and substances that chemically bind to this surface [19].

It is thought that electromagnetic enhancement results from localized surface plasmon resonances (LSPR) formed on rough metallic surfaces or on metal nanoparticles. LSPR is an optical phenomenon generated by light as a result of the interaction of incident light with conductive metal nanoparticles smaller than its wavelength. The electric field of the incident light excites electrons to the conduction band, and as a result coherent localized plasmon oscillations are obtained (Fig. 3.3). The resonance frequency of these oscillations depends on the composition, size and geometry of the nanoparticles dielectric environment and distance between the nanoparticles [11].

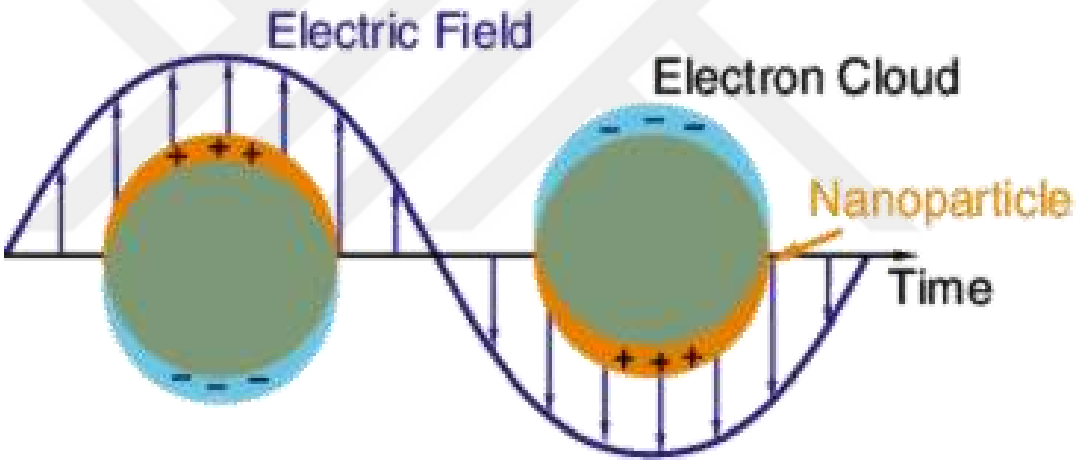

Figure 3.3. *Schematic representation of surface plasmon resonance localized around the metal nanoparticle. The coherent oscillations in the free electrons of the metal nanoparticle can be initiated by the oscillating electric field of the incident light. This initiated oscillating electric dipole greatly increases the scattering and absorption of resonant wavelengths compared to dielectric nanoparticles of similar size and becomes a superior method for use in single molecule detection [20].*

The increase in Raman signal is thought to be provided by hot-spots, composed of strong and highly localized electromagnetic fields caused by LSPR. Hot spots are enhanced electromagnetic field regions in between the molecules which are in appropriate and predictable locations [13]. The rapid change in SERS enhancement factors depending on hot-spot and relative position for a nanoparticle dimer is schematically shown in Fig. 3.4[11]. To obtain an optimum result from a SERS analysis, the analyte molecules must either be adsorbed

to the surface of the metal nanoparticles or be located in the near environment of these nanoparticles.

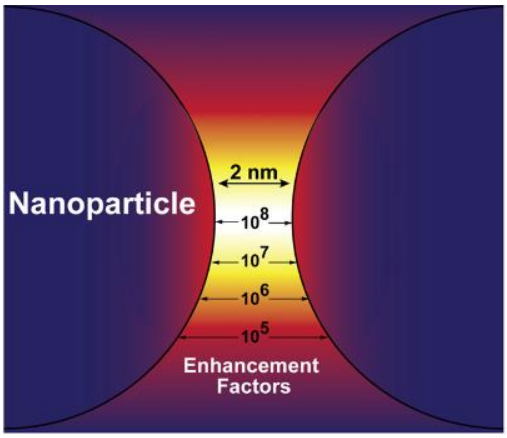

Figure 3.4. *Schematic representation of the rapid change in SERS enhancement factors according to the hot-spot and relative position for a nanoparticle dimer [11].*

The analyte molecules in the hotspots are strongly excited and emit amplified Raman signals. The SERS enhancement factor obtained by electromagnetic effect is generally between 10^6-10^{10}, whereas contribution from the chemical effect is only 10^2. These two mechanisms simultaneously contribute to the overall enhancement. However, the electromagnetic effect is thought to be the primary contributing mechanism [21].

3.4. Enhancement Factor

The enhancement factor (EF) is used to characterize SERS effect, in other words, to quantify the magnitude of amplification. EF is quantitatively related to the increase in signal intensity per molecule and depends on SERS conditions such as substrate, analyte and laser wavelength. It is impossible to make a single definition for EF due to the variety of situations (for example; single molecules, multiple molecules, experimental limitations such as not knowing the exact number of molecules, surface distribution of analyte molecules, etc.) that may arise in SERS. The three most important definitions of EF are single molecule EF, average EF in terms of SERS substrate and analytical EF from the analyte chemistry point of view [22]. For example, the average EF for SERS substrates is usually determined by the following equation:

$$EF = \frac{I_{\mathrm{SERS}}/N_{\mathrm{Surf}}}{I_{\mathrm{RS}}/N_{\mathrm{Vol}}} \quad (2.1.)$$

where I_{SERS} is total SERS intensity, I_{RS} is Raman (non-SERS) intensity $N_{\mathrm{Vol}} = c_{\mathrm{RS}}V$ is the average number of molecules in the scattering volume (V) for the Raman (non-SERS) measurement, and N_{Surf} is the average number of adsorbed molecules in the scattering volume for the SERS experiments [22].

When SERS EFs are correctly identified and measured, EF values in the range 10^7-10^8 are sufficient to detect single molecule-SERS signals. For a better SERS substrate, the surface of substrate must generate the strongest possible plasmon resonance (hence, maximum number of hotspots) possible [22]. Moreover, uniformity plays a crucial role on the efficiency of the SERS substrate. When the size, shape and aggregation state of metallic nanoparticles are uniform, the reproducibility of the results increases. In this case, the information obtained from SERS is more reliable and accurate [23].

3.5. SERS Substrate Production Methods

Numerous methods have been reported in the literature on the production of two-dimensional and three-dimensional SERS substrates. They are usually produced by bottom-up or top-down approaches, but it is also possible to use both approaches together. Nanostructures are synthesized from atoms or molecules in the bottom-up approach, while they are obtained by breaking down bulk materials in the top-down approach. SERS substrates produced using these approaches can be basically divided into three groups which are briefly described below.

3.5.1. Metallic electrodes

The first substrates that provided enhanced Raman signals for the molecules adsorbed to the surface were Ag electrodes whose surface was roughened by electrochemical methods [12]. Although these substrates played an important role in the development of SERS technique, their importance has gradually decreased with the development of substrates with higher enhancement effect. In addition, problems encountered with large scale production of these materials and unappropriate electrochemical processes limited the widespread use of these substrates [24].

3.5.2. Nanostructured platforms

These platforms are produced by using micro- and nano-fabrication techniques to obtain metal surfaces with nano-scale roughness [25].However, since lithographic techniques require expensive and complex devices, the high cost limits the use of these platforms in SERS applications are limited.

3.5.3. Colloidal metal nanoparticles

Colloidal metal substrates are widely used in SERS applications and preparation of these substrates does not require complex devices. SERS measurements are usually performed by mixing colloidal metal nanoparticles directly with the analyte and dropping them onto a suitable substrate such as silicon wafer or quartz plate followed by recording Raman spectrum after the drop is dried. In colloidal metal nanoparticles, liquid medium helps to transport molecules of analyte to plasmonic surfaces. However, it cannot be used effectively when the analyte is incompatible with the liquid medium [25]. The most common metals used in the production of these substrates are noble metals such as Ag and gold (Au). This is because the energy levels of the d-d transitions in these metals show LSPR in the visible spectrum. Ag gives the sharpest and strongest bands among all metals. In addition, Ag is the only metal that produces plasmon resonance in the entire visible spectrum [26]. However, the oxidation resistance of Ag is low. Therefore, Au may be preferred in some applications due to its non-reactivity (inertness) and biocompatibility [11].

4. SILVER NANOPARTICLES IN SERS APPLICATION

Silver nanoparticles (AgNPs) exhibit unique physico-chemical properties such as high electrical and thermal conductivity, catalytic activity, optical properties and antimicrobial activities which allows their utilization in various applications including optoelectronics, catalysis, biomaterials, biosensors and SERS [27,28]. When decreasing particle size to nanometer scale, percentage of atoms at the surface increases and a quantum effect appears. This is why the physical and chemical properties of nanomaterials is very different from those of corresponding bulk materials. At nanoscale, the color of AGNPs changes, as the particle size changes [29]. The origin of metal nanoparticles' colour is LSPR which strongly depends on the size and shape of metal nanoparticles. The solutions of spherical AgNPs are usually yellow. In other forms, particularly amorphous particles are generally opaque yellow and sometimes gray [30].

There are a variety of synthesis methods of AgNPs reported in literature. Among them, chemical reduction in solution phase is the most common method of synthesizing AgNPs. Basically, this methods includes three main components; a metal precursor (generally silver nitrate ($AgNO_3$), reducing agents (e.g., sodium borohydride ($NaBH_4$), glucose, trisodium citrate, formaldehyde etc.) and stabilizing agents (cetyltrimethylammonium bromide, polyvinylpyrrolidone, *etc*.) [19,28]. Although the method is easy to perform, synthesis of uniform and stable AgNPs with a controllable size is challenging.

The properties of AgNPs strongly depend on the morphology of particles; hence, it is crucial to be able to control the size and shape of nanoparticles. In recent years, AgNPs with different shapes (cubes, prisms wires, octahedrons, triangular, bars, *etc*.) were obtained [11]. The diversity of the shape of the AgNPs greatly changes the LSPR properties (Fig. 6) and thus their performance in SERS applications [30].

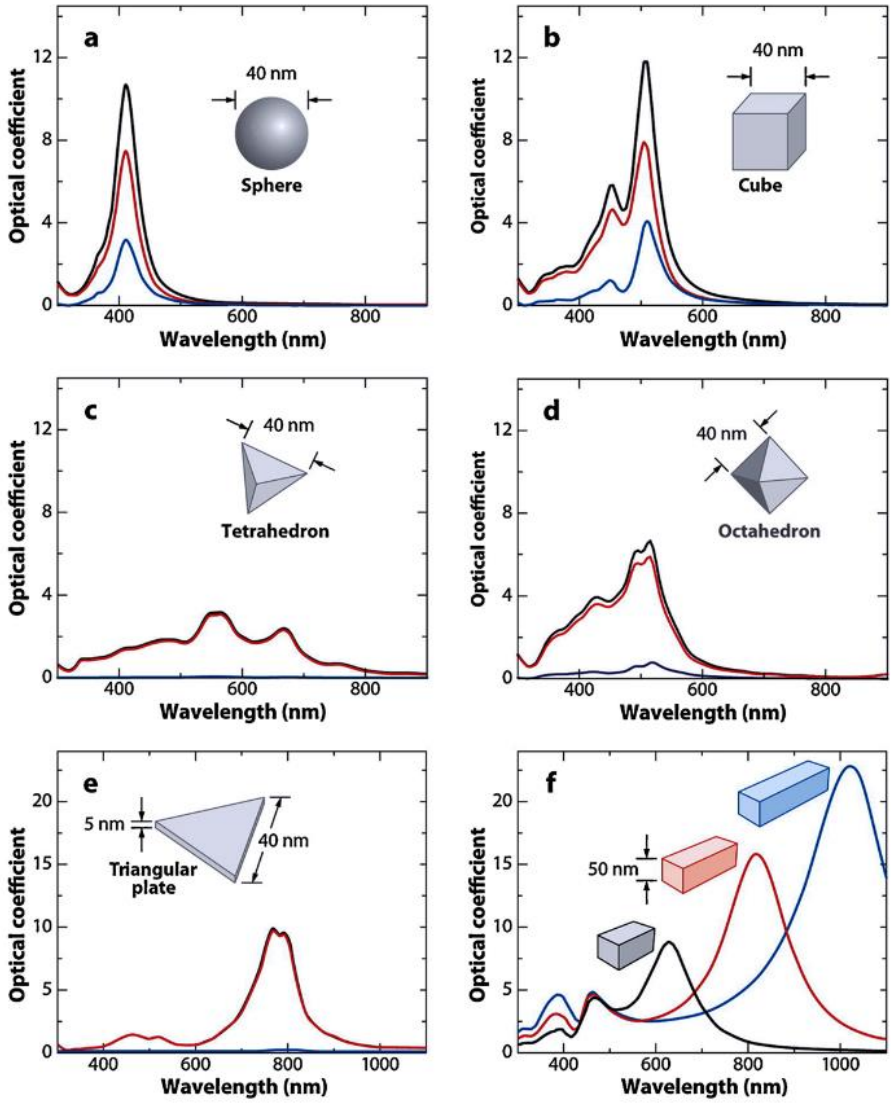

Figure 4.1. *Optical properties of silver nanoparticles in different shapes :a)a sphere, b)a cube, c)a tetrahedron, d) an octahedron, and e)a triangularplate; absorption is shown in red, scattering in blue, and extinction in black colour. (f)Extinction spectra of rectangular bars with aspect ratios of 2(black), 3(red), and 4(blue) [11].*

The size and shape of synthesized AgNPs are basically determined at nucleation and growth stages [31]. Thus, understanding the formation mechanisms of AgNPs is crucial to be able to perform a size and shape controlled nanoparticle synthesis.

The mechanism proposed by LaMer and Dinegar [32] in 1950 is still a basic model that shows the formation of nanoparticles in a solution phase. According to this model which is illustrated in Fig.4.2, the formation of nanoparticles from supersaturated solutions begins with

nucleation stage where atoms start to aggregate, forming small clusters and finally stable nuclei. The nucleation stage is followed by a growth stage, where the size of the seed increase via incorporation of metal atoms to the growth surface [33].

All nuclei are required to form at the same time for the synthesis of monodispersed AgNPs. In this case, all the nuclei are likely to have the same or similar size, and then they will have the same subsequent growth. The nucleation and growth stages can be controlled by changing the experimental conditions, such as reaction temperature, pH, concentrations of precursors, reducing and stabilizing agents [31].

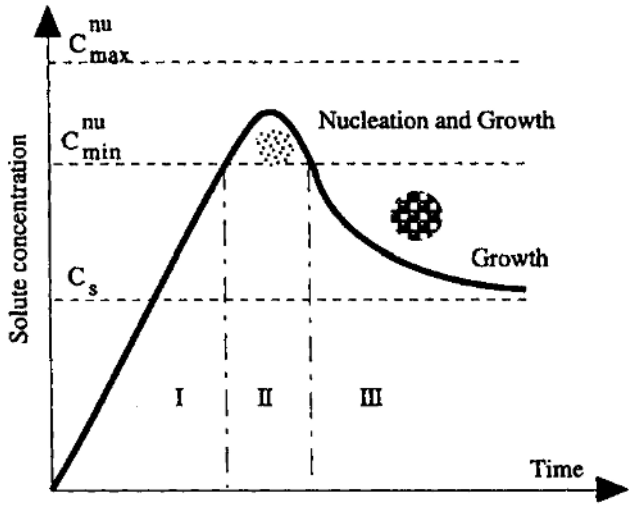

Figure 4.2. *LaMer model describing nucleation and growth of metal nanoparticles formation in solution phase [33].*

In 1951, Turkevich *et al.* [34] synthesized gold nanoparticles with a spherical shape and narrow size distribution by reducing the chloroauric acid with trisodium citrate ($Na_3C_6H_5O_7$ – denoted as TSC in this thesis study) in an aqueous solution while boiling. Later, this method was used for synthesis of silver colloids [35]. Lee and Meisel [35] synthesized AgNPs using sodium citrate to reduce silver nitrate ($AgNO_3$) at its boiling point. In contrast to relatively uniform gold nanoparticles, AgNPs synthesized in an aqueous solution by this method show variation in terms of size and shape (spheres, rod, prisms, plates). Nevertheless, citrate reduction method is still commonly used due to its simplicity.

In the TSC reduction method, the silver ion (Ag^+) produced by dissolving silver nitrate ($AgNO_3$) in water is reduced to a zero-valence state of silver (Ag^0, a free silver atom in solution) by the addition of TSC to the system. When concentration of Ag^0 reaches a certain value, the silver atoms starts to aggregate to form oligomeric clusters (such as Ag_2^+, Ag_4^+, Ag_9^+). The citrate ion can form relatively stable complexes with positively charged Ag_2^+ ions ($(Ag)_2^{+\cdots}(citrate)^-$). As the complexes slowly grow further by aggregation, they reach an optimal size, at which stage the strong repelling layer of citrate prevents them from coming into close contact and then grow via the reduction of Ag ions on their surface in order to form final colloidal stabilized AgNPs as illustrated in Fig 4.3 [19, 36, 37].

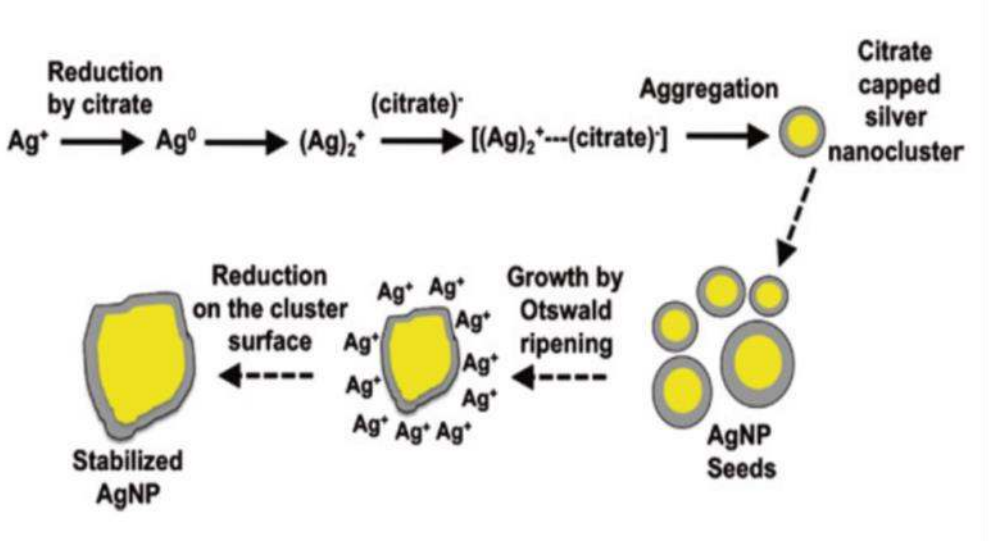

Figure 4.3. *Schematic illustration of nucleation and growth mechanisms for AgNP obtained by the citrate reduction method [19].*

5. CHALLENGES IN THE APPLICATION OF SERS TECHNIQUE AND APPROACHES DEVELOPED TO OVERCOME THESE CHALLENGES

Numerous studies have been performed on the development of high performance SERS substrates since SERS technique has a high potential in the fields of chemical and biological detection, food safety and medical diagnostics. While the reported SERS substrate production methods generally perform well, many are tedious, time-consuming, complex and costly methods [38]. Although there are many publications and patents which propose new SERS active materials, the number of commercially available substrates for use in routine analysis is very limited and very expensive. In addition, their stability is low. They must be stored in a controlled atmosphere and used with caution in order to maintain their enhancement properties [25]. For the SERS technique to be able to become a method for using in routine analysis, it is necessary to develop stable and low cost substrates that allow repeatable measurements.

Metals such as Ag, Au and Cu are the most commonly used materials in SERS applications due to providing high SERS signal increase. Au and Cu show inter-band absorption in the visible wavelength range, while in silver, inter-band absorption occurs in the ultraviolet wavelength range. Therefore, among these metals, the highest SERS increase for visible light is achieved with Ag [39]. Moreover, Ag has high plasmonic enhancement effect, low optical frequency shifts and low cost compared to other noble metals. However, AgNPs are chemically unstable (especially against oxidation). Therefore, morphological and chemical changes that may occur in the structure may lead to a decrease in Raman intensity, variable SERS signals and misinterpretation of experimental results [39- 41]. Several studies have been performed to increase the chemical stability of AgNPs. Some of these studies include coating of AgNPs with a protective layer such as TiO_2 [42], SiO_2 [43] and Al_2O_3 [44] to develop core-shell nanostructures.

The surface roughness of the metal substrate or the size of the metal nanoparticles (depending on the substrate used) also affect the strength of the surface plasmons and the ultimate signal increase. Therefore, the roughness of the metal surface or the size of the nanoparticles plays a critical role in obtaining a good SERS enhancement. If the surface is too smooth or flat, no effective surface plasmon formation occurs.

The dimensions of the roughness-forming structures are usually between 20-100 nm for the laser wavelengths in the range of 532-780 nm [45]. The difficulties encountered in controlling size, size distribution and shape of the nanostructures or nanoparticles efficiently make it difficult to take repeatable measurements [25]. As well as the size and shape of nanostructures/nanoparticles, surface chemistry also directly affects the interactions between the analyte and the nanoparticles. For example, positively charged analyte molecules bind to nanoparticles with negative surface charge by attractive forces, while in case of using a negatively charged analyte there will be limited interaction due to repulsion forces, as a result, it becomes difficult to obtain strong and reproducible SERS spectra [46]. In consequence, one of the biggest difficulties encountered in the application of SERS as a routine analysis technique is the selection of the most suitable substrate for the analyte [25].

Since colloidal nanoparticles are relatively easy to produce and do not require complex devices, they are promising for easy and cost-effective SERS measurements. The analyte molecules are easily captured by colloidal nanoparticles, allowing rapid analysis [9]. However, the SERS signal in these substrates strongly depends on the aggregation state of the colloids. Since the adsorbants affect the degree of aggregation, different analytes cause different intensities, making reproducibility and standardization difficult [24]. Furthermore, due to the coffee-ring effect caused by the capillary flow during drying of the analyte/colloidal nanoparticles mixture which was dropped onto the substrate, the dispersion of analyte and nanoparticles in the dried drop is not uniform [9]. Due to higher evaporation rate at the edges of the drop, there is a flow outward from the central of the drop (to compensate for the loss of solvent at the edges) and this flow drags a significant amount of particles and molecules with it and causes them to accumulate along the edges of the drop. The remaining components are dispersed randomly in the dried drop area. This uncontrolled distribution of analyte and nanoparticles makes it difficult to obtain repeatable and strong SERS spectra. Therefore, it is necessary obtain a more uniform analyte and metal nanoparticle distribution in the dried drop area [46].

Avcı and Culha [46] carried out the drying process in a case at which the droplet was suspended on a hydrophobic surface (surface was kept in the inverse position) in order to prevent coffee-ring effect. Since the gravitational force acting on the metal nanoparticle-analyte complexes in this configuration is predominant to the outward flow in the horizontal

direction, most of these complexes were collected at the tip of the droplet during drying and confined to a smaller area. This configuration increased reproducibility of the measurements and enhanced the SERS signal by 10 times. Li *et al.* [40] confined both aqueous and organic analyte solutions to a small area by producing superhydrophobic-oleophobic Ag nanowire platforms to prevent random distribution and dilution of liquids on the SERS substrate. Thus, the detection limit of toxins was reduced by 10^3-fold.

Another problem encountered in the detection of the analyte in the droplet is intensifying the evaporation in the droplet with the effect of the laser and consequently the SERS signal changes continuously throughout the measurement [9]. In order to improve SERS performance, two-dimensional (2D) porous platforms such as porous polymers [47], porous anodic aluminum oxide templates [48], porous silicon [49] and porous glass-ceramics [50] were used to support metal nanoparticles. The surface morphology that is specific to porous substrates supports hot-spot formation [9]. In non-porous substrates, the interaction between particle motion and evaporation of the solvent determines the final morphology of the evaporating colloidal drop. In porous substrates, the penetration of the solvent into the pores affects the way of this morphology formation. Pack *et al.* [51] deposited aqueous colloidal drops containing nanometer- and micrometer- sized particles on nano-porous anodic aluminum oxide substrates and found that the rate of penetration of the solvent into the substrate was much faster than both evaporation and particle motion on the contact surface, and the authors reported that the coffee-ring effect is prevented when the substrate fully absorbs the solvent.

Three-dimensional (3D) porous platforms are more advantageous over 2D porous platforms in terms of quick penetration of solvent, preventing coffee-ring effect and providing strong analyte-metal interaction in SERS applications [52]. Lu *et al.* [53] prepared 3D SERS substrates by annealing to form uniform AgNPs on the surface of silicon nanowires produced by metal-assisted chemical etching using AgNPs as catalysts. They found that formation of a thin compact SiO_2 layer with the formation of AgNPs in the silicon nanowires increased the stability of the SERS substrate. Vendamani *et al.* [54] obtained significant enhancements in the Raman signals by decorating the vertically aligned silicon nanowires with AgNPs and they observed that the intensity of SERS signal increases with an increase in the density of AgNPs decorated on silicon nanowires. However, methods used in these studies are complex, require

sophisticated equipments (a hydrophilic pretreatment (acetone, ethanol, piranha solution), hydrophobic post-treatment (HF solution), electroless deposition process) and time consuming.

At this point, expanded graphite (EG) could be a promising material to create 3D porous SERS substrates. EG has a highly porous worm-like structure and is produced by an abrupt heating of expandable graphite. Expandable graphite is a type of graphite intercalated compound and produced by treating natural graphite flakes by acid solutions and oxidizers [55]. Exposing expandable graphite to high temperatures causes the intercalants between graphene layers transform to gas form, resulting in an increase in the volume of the material up to 1000 fold [56]. As a result, graphene layers separate from each other. However, at some points they are attached to each other by weak Van der waals bonds and a structure consisting of multiple pores connected to each other is obtained. This process is schematically shown in Fig 5.1 [57].

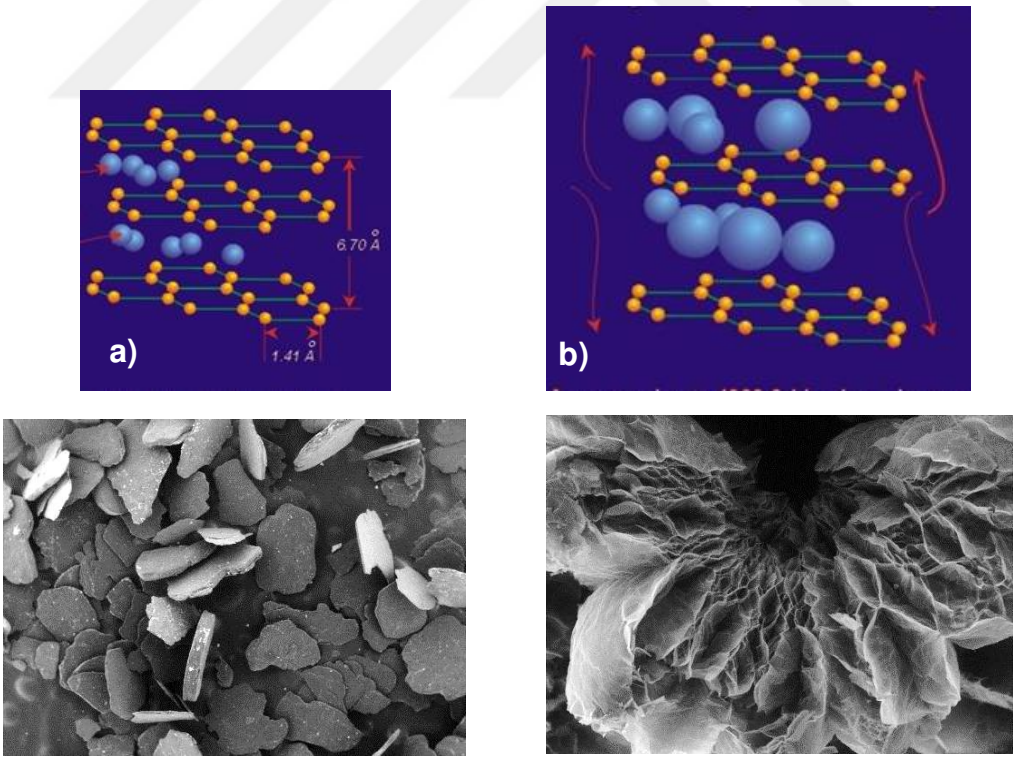

Figure 5.1. *Schematic representation of expansion process. a) The intercalated materials (blue spheres) as a liquid or solid phase remains trapped between graphene layers. b) Rapid heating causes the intercalated compound to expand which results in separation of adjacent graphene [57].*

In such a structure, the pores are predominantly macro-pore (pore width > 50 nm) that can reach up to µm. However, some meso-pores (pore width 2 - 50 nm) can also be found in the structure. The pore size and shape provide information on the degree of expansion of expanded graphite samples and can be controlled by process parameters such as temperature and expansion time [56].

EG has a very high specific surface area, high amount of porosity and functional groups on its surface that determine its absorption properties [58, 59]. Moreover, in the structure of EG, there are folded and wrinkled regions on the surface of the graphene layers. These regions lead to many nano-cavities where different particles can be located. Moreover, these metal particles can be protected from oxidation with the aid of graphene layers.

Graphene-based materials are promising for SERS applications due to their flexibility, excellent optical permeability, superior mechanical strength and most importantly, SERS enhancement through charge transfer mechanism (chemical effect) [38]. Recently, several studies have been performed on preparation of composites consisting of noble metal nanostructures and graphene-based materials (few-layer graphene, graphene oxide, reduced graphene oxide and CVD (chemical vapor deposition)-produced monolayer graphene) to increase the sensitivity, stability and reproducibility of SERS substrates. These studies were mostly focused on the effect of graphene on enhancing SERS signals. There are also studies for the use of graphene as a protective layer to enhance the stability of plasmonic metal surfaces. These studies showed that, due to its chemically inert nature and surface plasmonic properties, monolayer graphene synthesized by CVD [60], mechanically exfoliated graphene [61] and chemically exfoliated graphene oxide [62] could act as an ultra-thin protective layer for metal nanoparticles; consequently, stable and reusable SERS substrates could be obtained. Lee *et al.* [41] coated AgNPs with few-layer graphene and subjected them to intense heat treatment under environmental conditions and showed that the few-layer graphene inhibited oxidation of AgNPs. Suzuki and Yoshimura [39] reported that the SERS substrates prepared by growing the monolayer graphene by CVD method over AgNPs which were deposited on SiO_2 substrate exhibited SERS even in concentrated sulfuric acid and heated up to 400°C in air. These studies have shown that graphene can act as an ultra-thin barrier to improve the chemical stability of noble metal nanostructures, due to its chemical stability and its honeycomb lattice can completely inhibit the penetration of small molecules. Wang *et al.* [63]

reported that graphene /Ag nanocomposites that were produced by reduction of Ag ions in graphene dispersions obtained by exfoliation of EG in N-Methylpyrrolidone (NMP) by sonication can be used as an ultra-sensitive SERS substrate for chemical and biological analyses.

In this thesis study, it was hypothized that it can be utilized from the highly porous structure, high specific surface area and the presence of nano-cavities on the surface of expanded graphite to decorate AgNPs and these EG/AgNPs nanocomposites could be used as an efficient SERS substrate. **Accordingly, the aim of this thesis** was to investigate the performance of expanded graphite as a platform material to support metal nanoparticles and analyte molecules. It was proposed that 3D, metal nanoparticle decorated expanded graphite platforms would enable uniform distribution of metal nanoparticles and analyte molecules, and fast penetration of solvent, as well as utilizing from the Raman signal enhancement effect of graphene layers comprising the EG and from the ability of these graphene layers to protect metal nanoparticles from oxidation.

It should be noted here that when this thesis study was proposed and started to be performed in 2017, direct usage of EG (without exfoliation in a solvent) as a SERS substrate had not been shown in the literature. However, a very recent study, which was published in 2019 by an independent group, Sykam *et al*. [64] reported utilizing 2D flexible graphite sheets with a thickness of 0.3 mm as a SERS substrate. The authors mainly focused on the R6G dye adsorption capacity and SERS performance of these 2D flexible sheets. Although, they mention that incorporation of AgNPs into these substrates increases the SERS performance, they did not present these results in detail in this paper.

6. EXPERIMENTAL PROCEDURE

6.1. Silver Nanoparticle Synthesis Studies

6.1.1. Starting materials

AgNPs were basically prepared in water by a chemical reduction method. Silver nitrate ($AgNO_3$, cryst. extra pure, Merck) was used as a silver precursor. It is known that a variety of reducing agents are used for the synthesis of AgNPs by chemical reduction in solution phase [19]. Because of different reduction potential of these reducing agents, nanoparticles can be synthesized in different size, shape and distribution. In this study, AgNPs were synthesized by using three different reducing agents: trisodium citrate dehydrate ($Na_3C_6H_5O_7.2H_2O$, $\geq$ 99%), hydroxylamine hydrochloride ($NH_2OH.HCl$, 99%) and ascorbic acid ($C_6H_8O_6$, $\geq$ 99%), all supplied from Sigma Aldrich. Since any impurities would prevent controlled colloidal AgNPs synthesis, all glasswares were cleaned using 3M HNO_3 (65%) solution before synthesis processes. The glasswares were then thoroughly washed with deionized water and allowed to dry.

6.1.2. Synthesis of AgNPs using trisodium citrate (TSC) dehydrate as a reducing agent

In this approach, the synthesis of AgNPs were performed by using the procedure proposed by Lee and Miesel [35] and TSC dehydrate was used as a reducing agent. In order to synthesize colloidal AgNPs with desired shape, size and distribution, it is necessary to find the optimum synthesis conditions by considering different synthesis parameters such as concentration of reducing agent, pH and temperature. In this study, only the effect of the TSC concentration on the size and shape of AgNPs was examined using different TSC concentrations (10, 20, 34, 50 and 60 mM), while keeping the other parameters constant. In all syntheses, the concentration of the $AgNO_3$ was kept as $1.0x10^{-3}$ M. Basically, 50 ml $AgNO_3$ solution was heated under stirring until it begin to boil. Then, 5ml of TSC solution with a specific concentration was added dropwise to $AgNO_3$ solution. After a color change was observed in solution, heating and vigorous stirring were continued for an additional 15 min. The solution was then cooled naturally to room temperature and stored at 4°C for further use and characterization. No reflux system was used in this study.

6.1.3. Synthesis of AgNPs using hydroxylamine hydrochloride (HH) as a reducing agent

In this approach, the synthesis was performed according to the method proposed by Leopold and Lendl [65]. Briefly,10 ml of 10^{-2} M $AgNO_3$ aqueous solution was rapidly added to 90 ml of hydroxylamine hydrochloride (denoted as HH) aqueous solution (1.67 x 10^{-3} M) containing $3.33x10^{-3}$M NaOH and stirred for 20 min at room temperature. The colour change of the solution to orange-brown indicated successful nanoparticle formation. Prepared colloidal silver dispersion prepared by this approach was denoted as "*$AgNO_3$ added to HH/NaOH* ". In some of the studies reported in the literature, centrifugation was applied after synthesis in order to remove undesirable by-products [66, 67]. To observe the effect of centrifugation process, 20 ml of as-synthesized dispersion was centrifuged at 5000 rpm for 30 min. Then, the supernatant was removed by pipetting and the sediment was redispersed in deionized water. Then, centrifugation process was repeated at the same conditions. After the second centrifugation, the supernatant was removed and the sediment was redispersed in deionized water and this dispersion was denoted as "*centrifugated* ". 20 ml of centrifugated product was sonicated in ultrasonic bath for 30 min in order to see the effect of sonication process and was denoted as "*sonicated* ".

This AgNPs synthesis approach was also performed by changing the order of the addition squence of chemicals into the reaction mixture as suggested by Leopold and Lendl [65] to see how the size and size distribution of AgNPs will be affected. For this purpose, 5 ml of $3x10^{-2}$ M NaOH aqueous solution was added into 5ml of $1.5x10^{-2}$ M HH aqueous solution, then the whole mixture was added into 90 ml of $1.11x10^{-3}$ M $AgNO_3$ aqueous solution while stirring. The mixed solution was stirred for further 20 min. The colloidal dispersion obtained at the end of the synthesis had a pH close to 7. The resulting dispersion showed a milky gray color, indicating the formation of nanoparticles and was denoted as "*HH/NaOH added to $AgNO_3$* ".

6.1.4. Synthesis of AgNPs using ascorbic acid (AA) as a reducing agent

In this approach, AgNPs were synthesized by the method described by Quin *et.al* [68]. The synthesis of AgNPs was carried out by using ascorbic acid (denoted as AA) as a reducing agent and TSC as a stabilizing agent. Initially, the pH of 100 ml of an aqueous solution containing $6x10^{-4}$ M AA and $3x10^{-3}$ M TSC was adjusted to 10 by adding 0.1 M NaOH

aqueous solution. Then, 1 ml of 0.1 M $AgNO_3$ aqueous solution was added dropwise and color change was observed in solution immediately. After mixing of solution for 15 min, the product was transferred into 100°C water bath and kept there for 30 min with stirring.

6.1.5. Characterization of the synthesized AgNPs

UV−visible analyses of colloidal AgNPs were carried out by using Shimadzu UV-3600 spectrophotometer in the 300−800 nm wavelength range. Prior to UV analyses, AgNPs synthesized with TSC were directly placed into the quartz cuvette, whereas AgNPs synthesized with HH and AA were diluted three times with deionized water and then placed into quartz cuvettes. The morphology of the synthesized AgNPs was examined using field emission gun scanning electron microscope (FEG-SEM, Zeiss Supra 50VP) operating at an accelerating voltage of 20 kV. Samples were prepared by dropping 10µL dispersion consecutively twice onto Si wafer with an oxide layer with a thickness of 300 nm and allowed to dry at room temperature. The Si wafer was cleaned with acetone and then isopropyl alcohol for 10 minutes in an ultrasonic bath and dried with N_2 blowing prior to dropping sample onto it.

6.2. Preparation of AgNPs Decorated Expanded Graphite (EG) Materials

0.5 g of commercially available expandable graphite (Expansion ratio:307, Grade 3772, Asbury Carbons Inc.) was put in an alumina crucible and placed into a preheated furnace at 1000°C for 2 min in order to prepare expanded graphite (EG). The sample kept in a vacuum desiccator until use. 100 ml of AgNPs colloidal suspension was sonicated in an ultrasonic bath for 30 min in order to disperse agglomerates. Then, sonicated AgNPs colloidal suspension and 0.5 g EG were placed in 500 ml flask and gently mixed with plastic spatula. After that, the flask was placed into rotary evaporator in order to removw water and coat EG particles with AgNPs. The obtained EG/AgNPs nanocomposite powder was then kept in an oven at 100ºC to remove residual water.

6.2.1. Characterization of AgNPs decorated EG materials

Phase analysis of EG/AgNPs nanocomposites were performed using X-ray diffractometer (XRD, Rigaku miniflex 600) at a voltage and current of 40 kV and 15 mA,

respectively. The XRD data were recorded between 10 to 80º 2θ values with a rate of 2º/min. The microstructure of the samples were characterized by FEG-SEM (Zeiss Supra 50VP) operating at an accelerating voltage of 15 kV. Energy-dispersive x-ray spectroscopy (EDX) analyses of these samples were also performed.

6.3. Preparation of SERS Substrates

EG/AgNPs nanocomposite powders were compacted by an uniaxial press at a pressure of 20-30 MPa to form 3D porous pellets with a diameter of 1.3 cm and thickness of 3 mm. No additives were used during this compaction and the porous nature of EG material was preserved while creating these 3D-SERS platforms.

SERS activity of the prepared substrates were tested using Rhodamine 6G (R6G – $C_{28}H_{31}N_2O_3Cl$) (99%, Acros Organics) as a standard analyte. R6G solutions with different concentrations (10^{-3} to 10^{-12} M) were prepared by serial dilution technique using deionized water. SERS measurements were performed by drop casting of 20 µl of analyte solution onto the substrate. Due to the 3D porous structure of the substrates, the drop was penetrated into it within a few minutes and the corresponding Raman spectra could immediately be recorded by Renishaw inVia Raman microscope with a laser excitation wavelength of 532 nm, 10mW laser power and 2s acquisition time. 100x objective was used in SERS measurements.

7. RESULTS AND DISCUSSION

7.1. Silver Nanoparticle Synthesis

Enhancement of SERS signals strongly depends on the shape, size and aggregation state of AgNPs since these parameters influence the degree of SPR. AgNPs with a size in the range of 20–100 nm are suitable for SERS detection. In this study, AgNPs were synthesized by using three different reducing agents: trisodium citrate (TSC) dehydrate, hydroxylamine hydrochloride (HH) and ascorbic acid (AA).

7.1.1. Synthesis of AgNPs using trisodium citrate (TSC) dehydrate as a reducing agent

Figure 7.1 shows the photograph of colloidal AgNPs synthesized at different TSC concentrations. The colorless $AgNO_3$ solution was transformed from pale yellow to orange-yellow when TSC concentration was increased from 10m M to 60mM. The color formation indicates the creation of AgNPs. In AgNPs, the conduction band and valence band lie very close to each other so that electrons move freely. These free electrons give rise to surface plasmon resonance (SPR) absorption, occurring due to collective oscillation of electrons of AgNPs in resonance with incident light wave [30, 69].

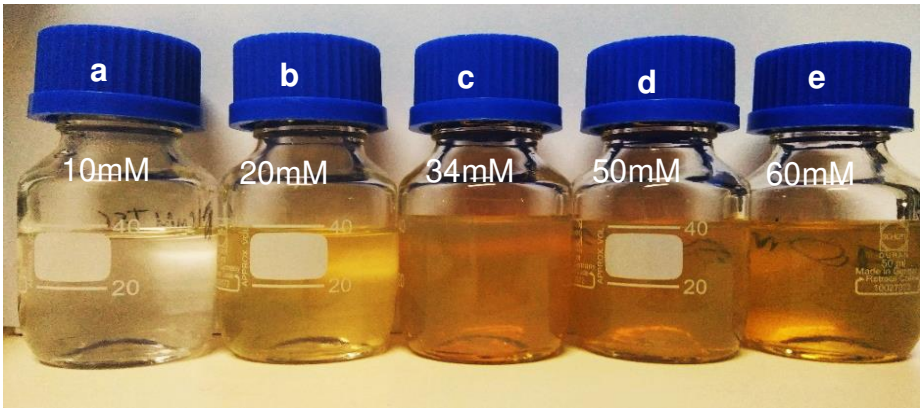

Figure 7.1. *Colloidal AgNPs synthesized at different TSC concentrations: a) 10mM, b) 20mM, c) 34mM, d) 50mM, e) 60mM.*

UV-Vis spectroscopy is one of the most commonly used techniques in the characterization of nanoparticles. It is known that the UV-vis spectrum is very sensitive to

AgNPs formation. Figure 7.2. shows UV-vis spectrum of AgNPs synthesized at different concentrations. It can be seen that absorption peak of AgNPs synthesized in the presence of 20, 34, 50 and 60mM TSC is observed at 427, 440, 435 and 429 nm, respectively. Previous studies [70, 71] showed that the SPR peak observed at 400-450 nm confirms the presence of AgNPs. The theory developed by Mie are used to calculate the SPR spectra (including both scattering and absorption) of a spherical particle of any size. According to this theory, spherical nanoparticles exhibit a single surface plasmon band [72]. It can be seen in Fig 7.2, SPR band of the dispersions includes only one peak, indicating that the synthesized particles are in spherical shape. The sample synthesized with 10mM TSC has a quite low extinction intensity due to the large particle size and aggregation, while other samples have obvious peaks due to the plasmon resonance of AgNPs. This indicates that 10mM TSC concentration is not enough to reduce the Ag^+ ions. When 20 mM TSC is used, a broad absorption spectrum is observed. This indicates that a wider size range exists in the synthesized AgNPs. Increasing the TSC concentration to 34mM was resulted in an absorption peak at 440 nm and an increase in intensity. This indicates that a higher amount of Ag^+ is reduced to metallic Ag. When the TSC value is used more than 34mM, the absorption peak slightly shifts to blue wavelengths due to formation of relatively smaller AgNPs. However, the absorbance of 50 mM TSC and 60 mM TSC added samples is less intense than that of the34mM TSC containing sample. This can be attributed to a decrease in concentration of AgNPs in the suspension with increasing TSC concentration. Since absorbance is the amount of light absorbed by the particles [73], the absorbance value in the UV-vis spectrum is directly proportional to the concentration.

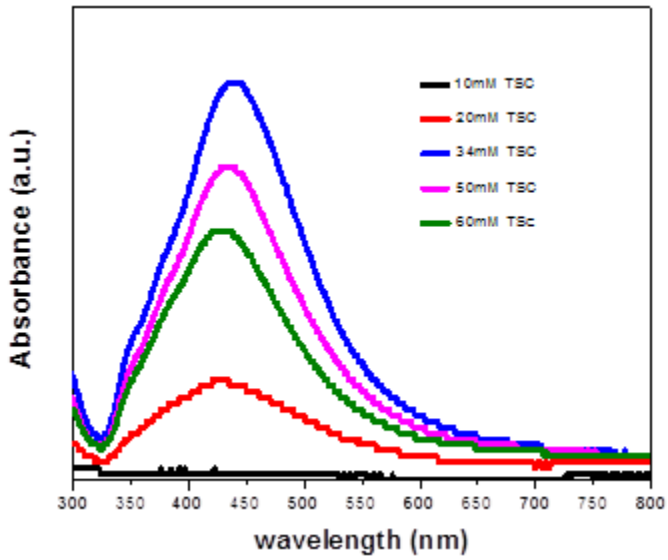

Figure 7.2. The UV-vis absorption spectrum of AgNPs synthesized at different TSC concentrations.

The size and shape of synthesized nanoparticles were examined by SEM. Figure 7.3 shows SEM micrographs of nanoparticles obtained by using different TSC concentrations. These images reveal that the formed particles are spherical. It has been reported in the literature that AgNPs synthesized by this approach have a wide variety of sizes and different shapes including rods, spheres and prisms [71,74]. However, in this study AgNPs with a spherical shape were obtained, although they have a relatively large particle size distribution. TSC acts as both a reducing agent and a stabilizing agent in this method. This complicates the determination of optimum TSC concentration; because a variation in its concentration may cause both a change in the reduction rate and in the nucleation and growth kinetics of particles. Stability of a solution of suspended particles such as colloidal AgNPs, is provided by electrostatic interactions. The diffuse layer around an electrostatically stabilized colloidal particle repels two colloidal particles when their double layers overlap, thereby stabilizing them against coagulation [29]. Negatively charged citrate ions ($C_6H_5O_7^{-3}$) electrostatically stabilized to AgNPs surface builds a double layer, repelling similarly coated AgNPs to avoid aggregation [75]. However, at low TSC concentrations (10 and 20 mM), coalescence of silver clusters occurs due to presence of insufficient citrate ions to prevent clusters from interacting with each other (Fig 7.3(a) and (c)). At high citrate concentration (60 mM), the ionic strength

of the solution increases and citrate layers destabilizes and consequently, many particles coalesce (Fig 7.3(i)). These results are in agreement with other published data [76, 77].

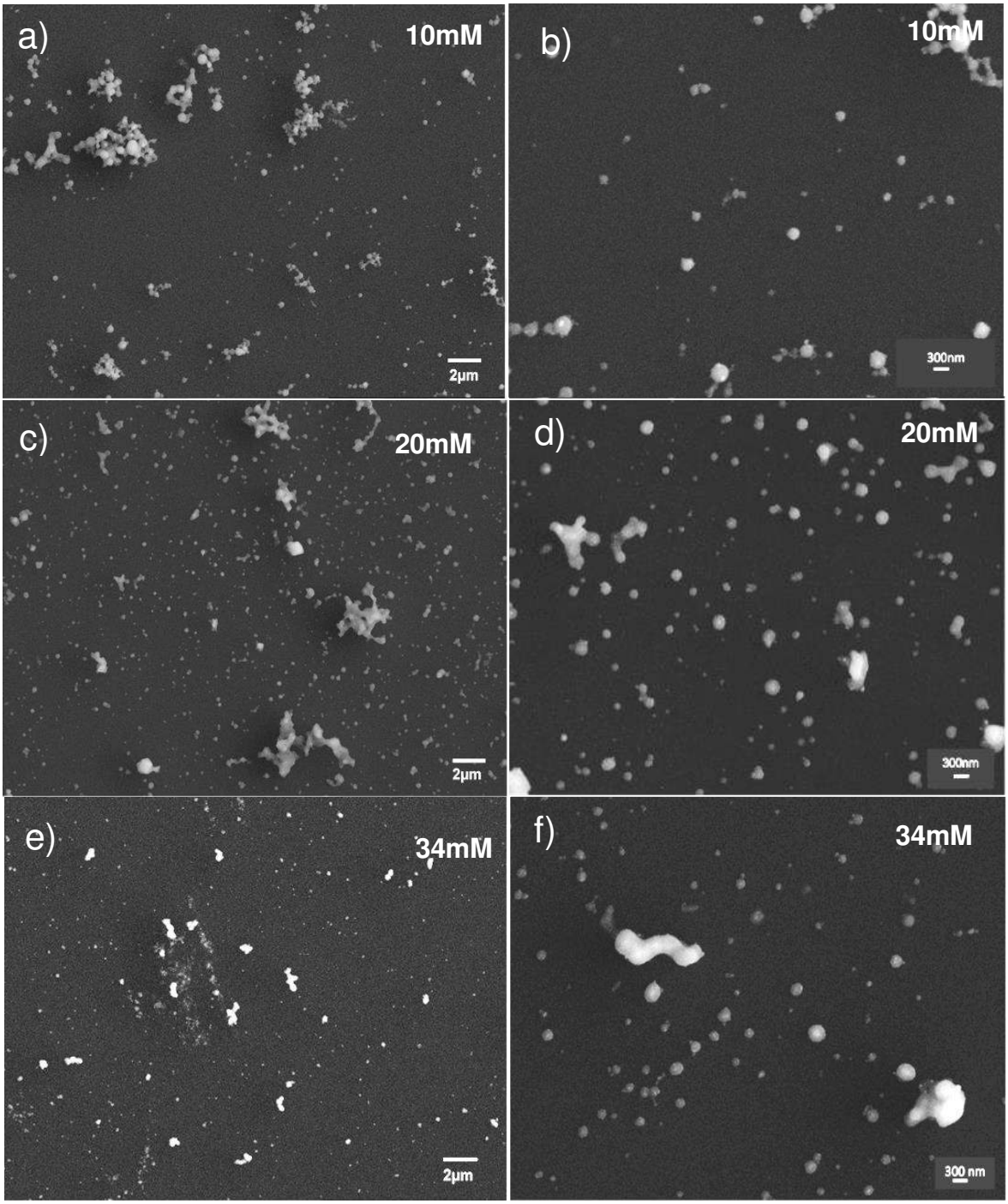

Figure 7.3. *FEG-SEM images of AgNPs synthesized at different TSC concentrations: a)10mM at low magnification, b)10mM at high magnification, c)20mM at low magnification, d)20mM at high magnification, e)34mM at low magnification, f)34mM at high magnification.*

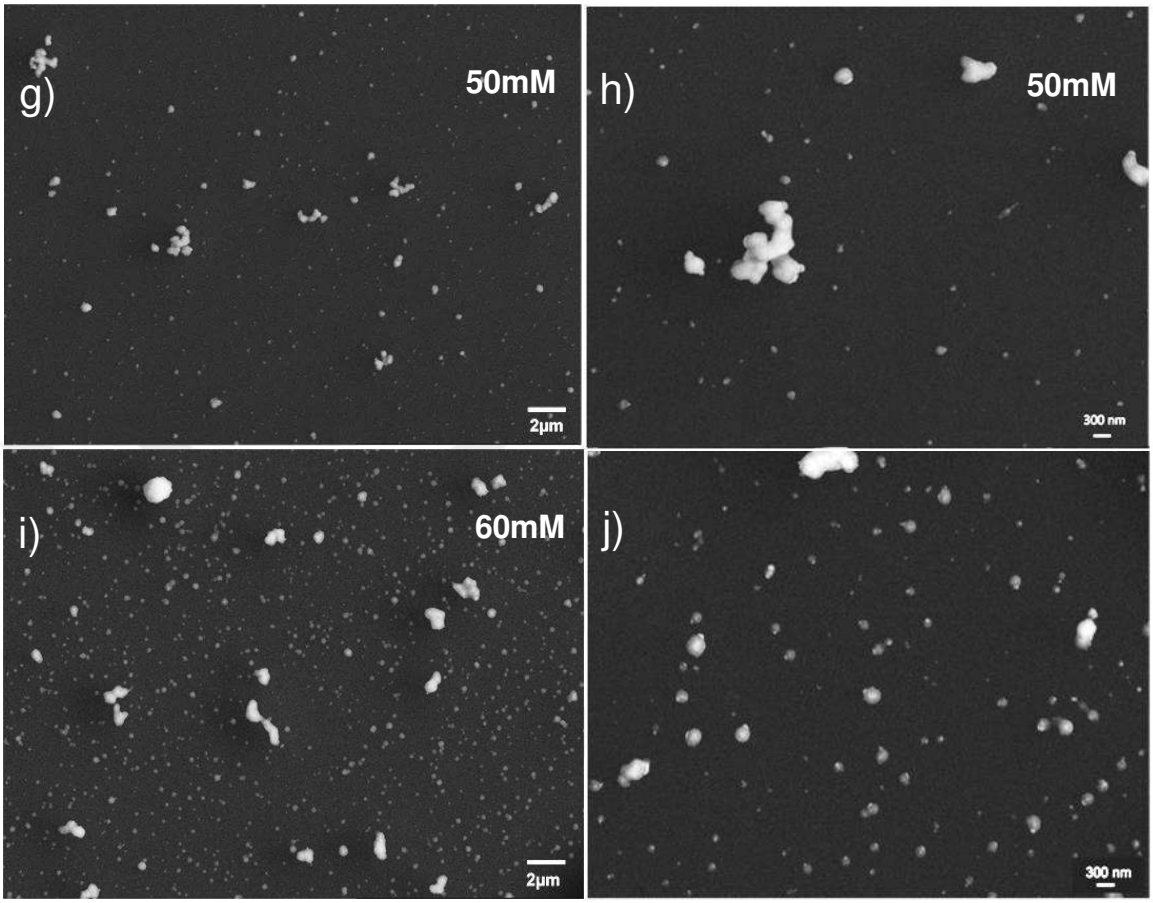

Figure 7.3. (Cont'd) *FEG-SEM images of AgNPs synthesized at different TSC concentrations: g) 50mM at low magnification, h) 50mM at high magnification, i) 60mM at low magnification, j) 60mM at high magnification.*

Image J software was used to analyze the particle size distribution of AgNPs. For each sample, 50 particles were randomly selected for size measurement. Agglomerations were not taken into consideration. Accordingly, 12% of these particles are in the size range of 44-100nm, while the size of 88% of them are > 100 nm, when the synthesis was performed with 10mM TSC. For the case of 20mM TSC, 35% of the particles are in the size range of 42-100 nm and 65% of them are > 100 nm. When the synthesis was performed with 34mM TSC, 42% of the particles are in the size range of 28-100 nm and 58% of them are > 100 nm. For 50mM TSC, 60% of particles are in the size range of 41-100 nm and 40% of them are > 100 nm. When 60mM TSC was used, 56% of the particles are in the size range of 32-100nm and the

rest is > 100 nm. The corresponding histograms for the particle diameters is given in Figure 7.4.

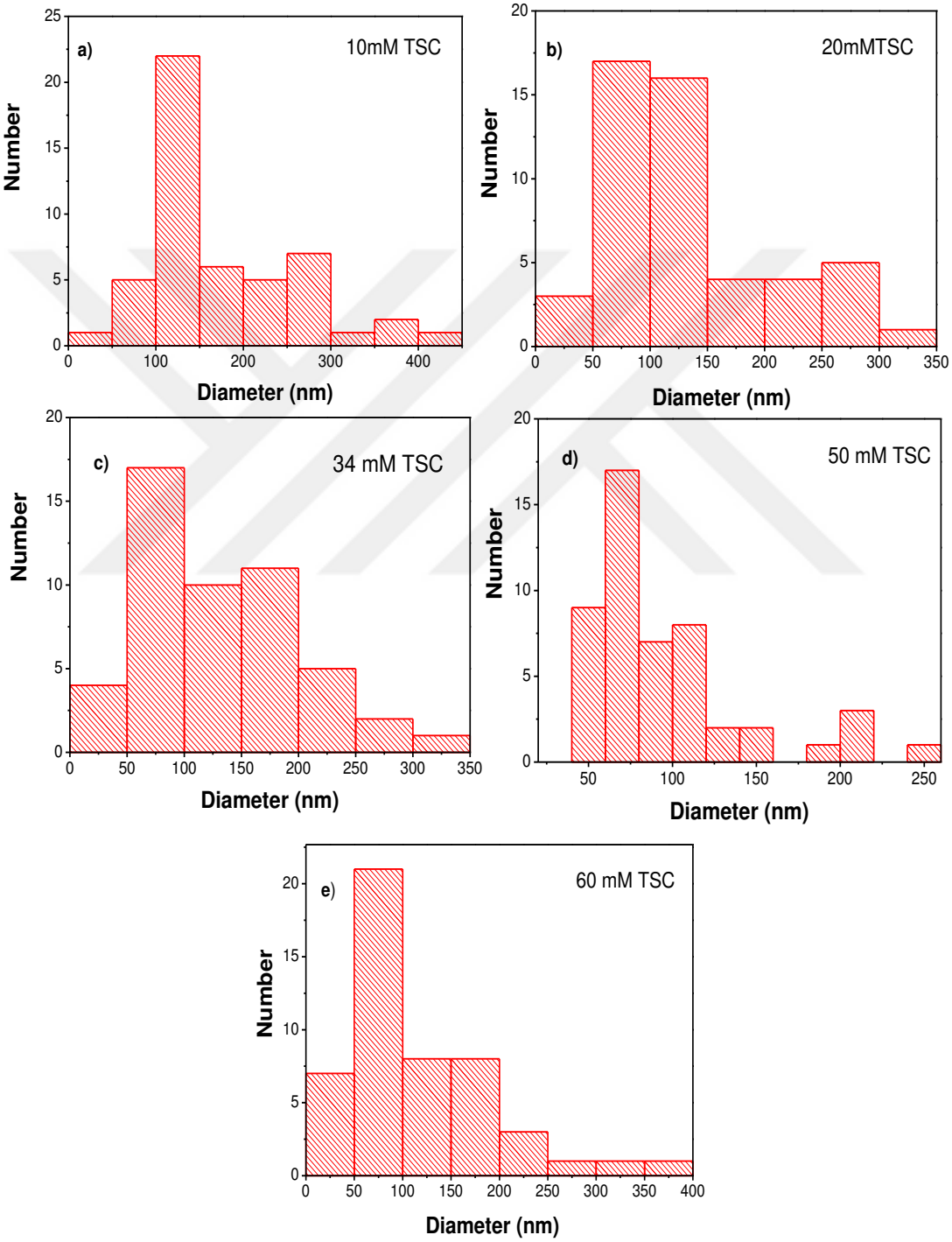

Figure 7.4. Size distributions of particles synthesized at different TSC concentrations: a) 10mM, b)20mM, c)34mM, d)50mM, e)60mM.

According to the SEM images in Fig 7.3 and statistical histograms of particles in Fig 7.4, it was concluded that AgNPs synthesized with using 34 and 50 mM TSC are more appropriate for further SERS studies. Very small nanoparticles cannot form plasmon since the number of electrons are not sufficient for collective excitation. This situation also applies for very large nanoparticles multipoles which are non-radiative in nature are excited [78]. So, SERS efficiency decrease as particle size increases, especially for very large particles [79]. Therefore, AgNPs synthesized with using 10, 20 and 60mM TSC are not suitable for SERS studies.

7.1.2. Synthesis of AgNPs using hydroxylamine hydrochloride (HH) as a reducing agent

Synthesis of AgNPs using HH as a reducing agent is relatively easier than synthesis by citrate reduction, since the reduction process can be done at room temperature. It should be noted here that the absorption spectrum may vary from batch to batch and this could be important in quantitative analytical detections. It is important that the synthesis is performed under the same conditions otherwise repeatable syntheses cannot be performed.

The UV-vis absorption spectrum of AgNPs synthesized by using HH is shown in Figure 7.5. When $AgNO_3$ solution added to HH/NaOH solution, the maximum absorption peak was found at 410 nm. When mixing order is changed (HH added to $AgNO_3$), the maximum absorption was shifted to 428 nm. These results are consistent with those reported by Leopold and Lendl [65]. It can be seen that the sonication process does not have a significant effect on the absorption intensity, but for the "centrifugated" sample (the precipitate) the intensity decreased and higher wavelength side exhibited a long tail. A quite broad absorption spectrum indicates that the size of those particles are much larger.

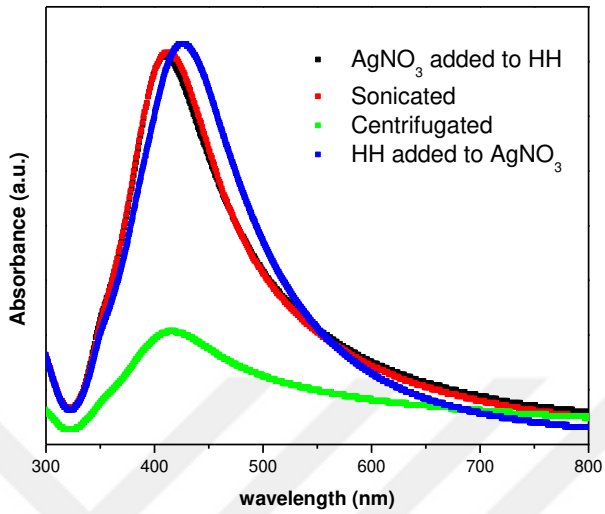

Figure 7.5. *UV-vis absorption spectrum of AgNPs synthesized by using hydroxylamine hydrochloride as a reducing agent.*

As shown in Fig 7.6(a), synthesized AgNPs formed agglomerations when $AgNO_3$ solution added to HH/NaOH solution. When centrifugation process was applied, mostly very large (a few μm) agglomerates were remained in the precipitate (Fig. 7.6(b)). When the SEM and UV-vis absorption spectrum of the "centrifugated " sample are analyzed together, it was concluded that the concentration of AgNPs with < 100 nm in diameter is extremely low. So, it was decided not to apply centrifugation in this approach for further studies. Figure 7.6(c), shows a large number of spherical AgNPs. Also, some agglomerates are observed. These results are in agreement with the results of Canameres *et al*.[80].

The statistical histogram of the particles (for 50 particles) synthesized by using HH as a reducing agent is shown in Fig. 7.7. For the case of $AgNO_3$ solution added to HH/NaOH solution, 44% of total particles are in the size range of 48-100nm, while those with sizes of 101-400 nm accounted for 56% of the total particles. The average particle size of this sample (individual paritcles) is 111 nm. When HH/NaOH solution added to $AgNO_3$ solution, 96% of the particles are in the range of 21-100 nm and 4% are in between 101-112 nm in size. The average particle size value of the AgNPs in this sample is 68 ± 24 nm, These results are in good agreement with the results obtained by FEG-SEM images. Accordingly, addition of HH/NaOH solution to $AgNO_3$ solution provided an appropriate particle size and size distribution of AgNPs for SERS analyses. The AgNPs synthesized by this approach may

exhibit good performance in SERS experiments since this sample also contains a certain amount of agglomerates.

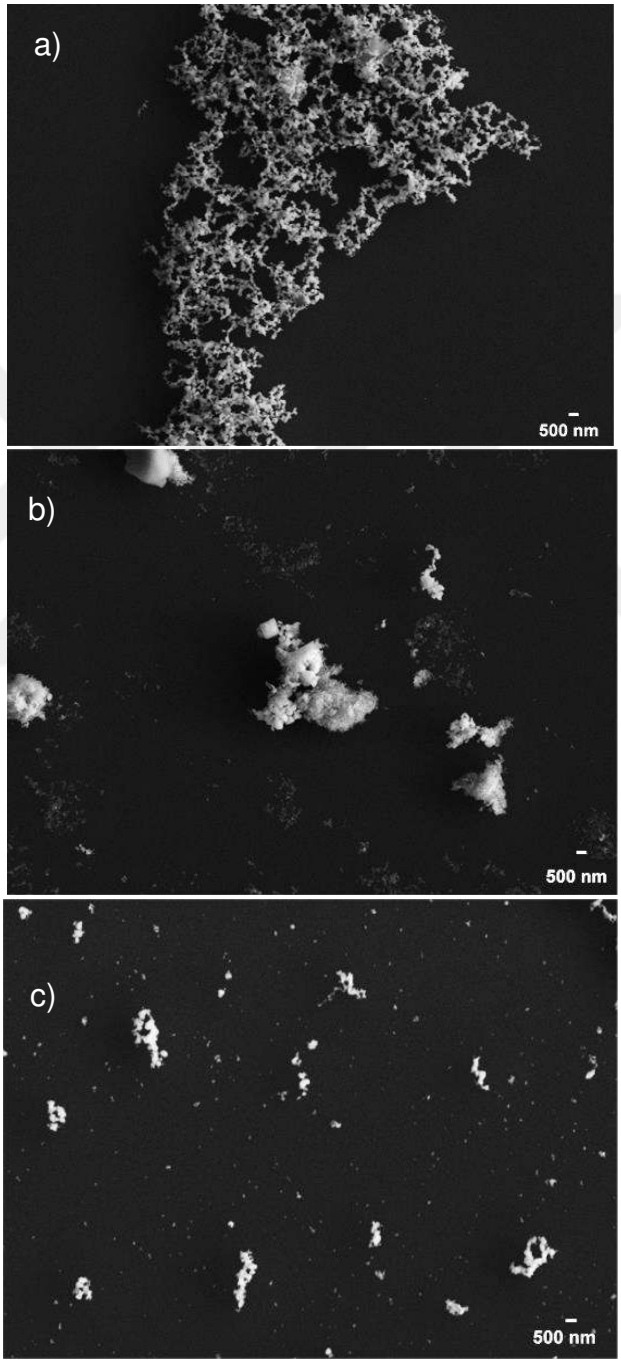

Figure 7.6. *FEG-SEM images of AgNPs: a) $AgNO_3$ added to HH/NaOH b) centrifugated, c) HH/NaOH added to $AgNO_3$.*

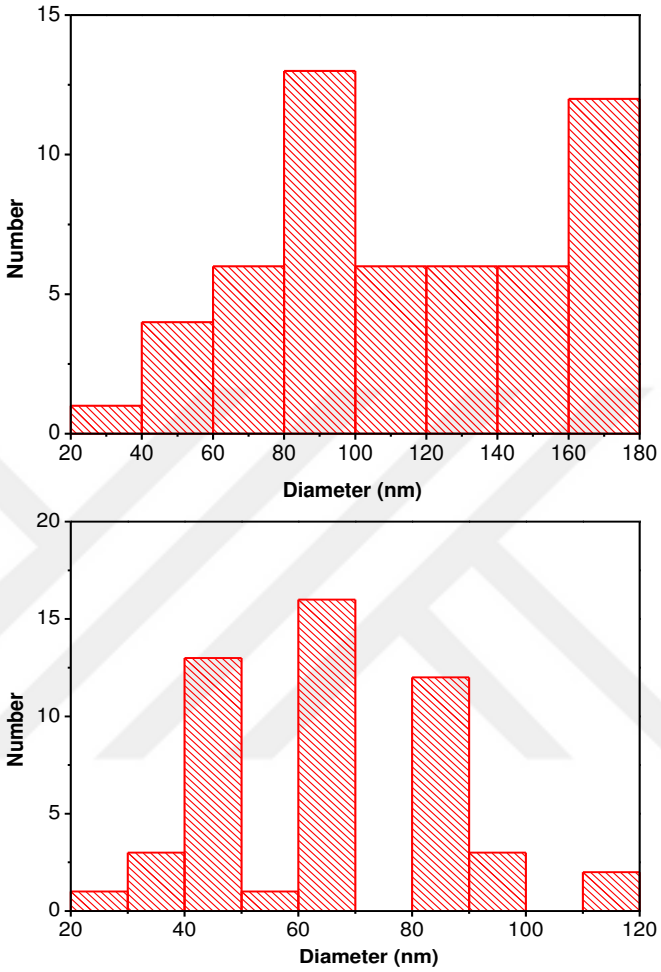

Figure 7.7. *Size distributions of particles synthesized by using HH as a reducing agent a) $AgNO_3$ added to HH/NaOH , b) HH/NaOH added to $AgNO_3$.*

HH synthesized AgNPs have negative surface charge due to chloride ions adsorbed on their surface which is represented by the electric double layers displayed in Fig. 7.8 [81]. To achieve optimal results from SERS analysis, effective adsorption of the analyte molecule to the SERS substrate surface is required. HH synthesized AgNPs are negatively charged and thus attracts positively charged Rhodamine 6G analyte molecules to be used as test probe in further SERS experiments.

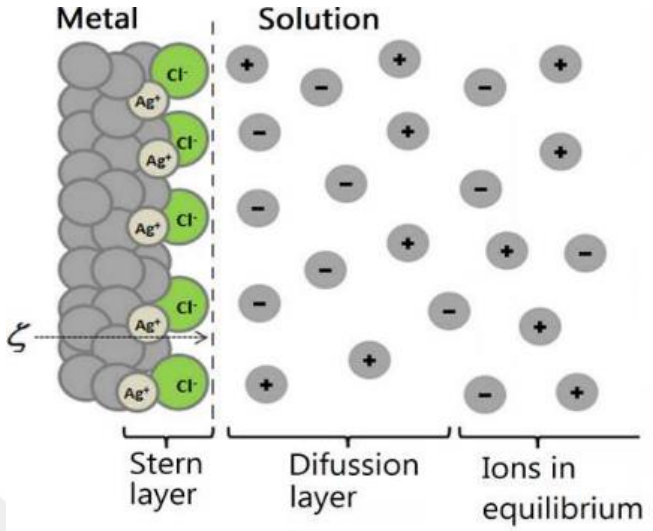

Figure 7.8. *Electrical double layer of Leopold Lend silver colloid [81].*

7.1.3. Synthesis of AgNPs using ascorbic acid (AA) as a reducing agent

AA serves as reducing agent and TSC as stabilizing agent in this approach. In comparison with the citrate reduction, the reaction is much faster and the color change is observed immediately when AgNPs synthesized by AA as a reducing agent. Because AA is a stronger reducing agent than TSC [82]. Figure 7.9 shows the UV-vis absorption spectra of the AgNPs synthesized by using AA as a reducing agent. The absorption peak of AgNPs was observed at 437 nm and it is narrow and symmetric, exhibiting no shoulder in the region of higher wavelengths, which suggests that the suspension has a narrow particle size distribution and does not contain much agglomerates.

Figure 7.10 shows the FEG-SEM images of AgNPs synthesized by using ascorbic acid as a reducing agent. The size distribution of the AgNPs is relatively narrow and shape of AgNPs is spherical as in agreement with UV-vis absorption results. This can be attributed to the equilibrium between nucleation and growth processes, and also to the increase in the reduction rate of the Ag^+ ions [83].

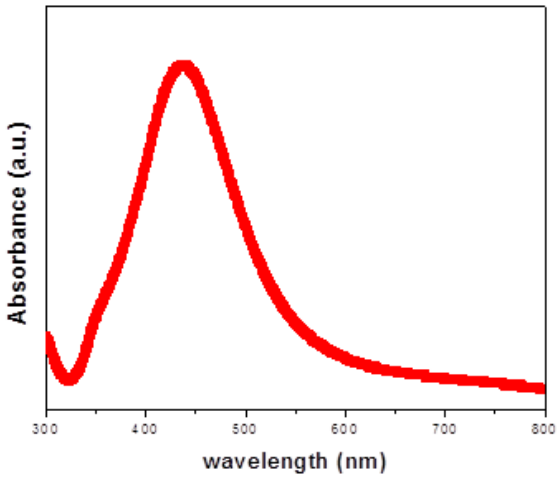

Figure 7.9. *UV-vis absorption spectra of AgNPs synthesized by using AA as a reducing agent and TSC as a stabilizer.*

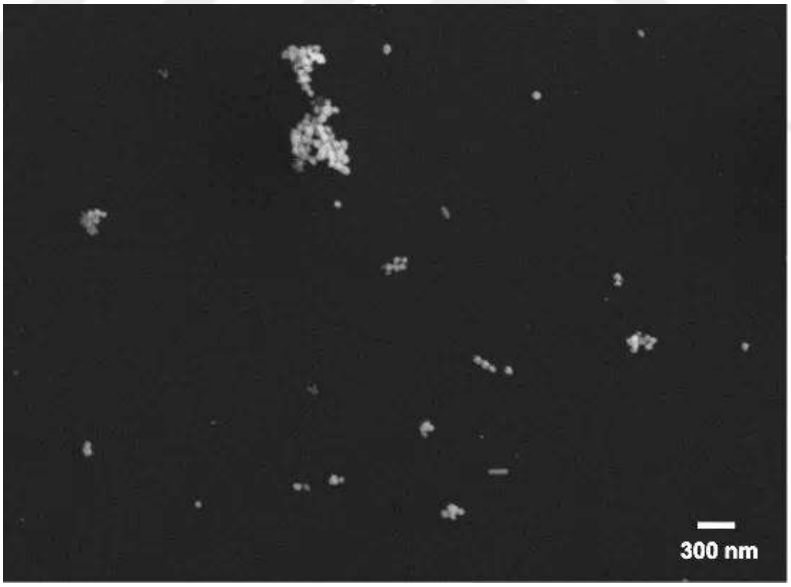

Figure 7.10. *FEG-SEM image of the AgNPs synthesized by using ascorbic acid as a reducing agent and TSC as a stabilizer.*

Using ImageJ software, the diameters of the 50 nanoparticles were measured. The statistical histogram of the AgNPs synthesized by using AA as a reducing agent is shown in Fig. 7.11. Accordingly, 100% of the particles are in the size range of 25-70nm and average particle size of the AgNPs is 52 ±9 nm. According to Lamer model [84], particle size can be controlled by rapid nucleation followed by slow growth. When TSC is used as a stabilizing

agent, it hinders the formation of more nuclei and so that controlled growth can be obtained. Thus, the particle size can be controlled. The LSPR and size distribution characteristic of AgNPs obtained in this study are in agreement with those reported by Qin et al. [68].

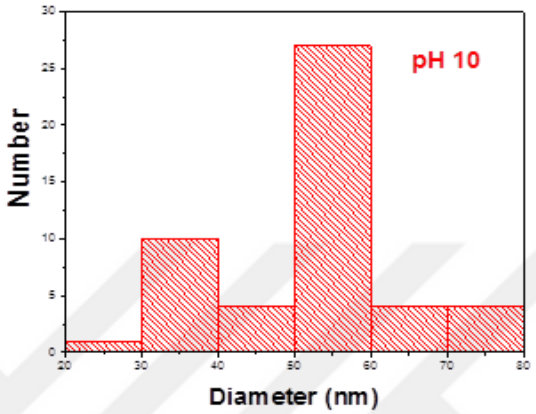

Figure 7.11. *Size distributions of particles synthesized by using AA as a reducing agent and TSC as a stabilizer.*

7.1.4. Comparison of the AgNPs synthesis approaches applied in this study

The UV-vis absorption spectrum of AgNPs synthesized by using three different approaches: trisodium citrate dehydrate, hydroxylamine hydrochloride and ascorbic acid is shown in Fig 7.12. Table 7.1 summarizes the average particle sizes and degree of agglomeration of the AgNPs prepared by these approaches. It is known that the microstructure and roughness of surfaces can have an important effect on SERS activity. The AgNPs synthesized by using AA may exhibit good performance in SERS experiments since these nanoparticles have small agglomerations and more spherical than the AgNPs synthesized by using TSC or HH.

Table 7.1. *Comparison of AgNPs synthesized by using three different approaches*.

	Average Particle Size (nm)	Particle Shape	Degree of Agglomeration
TSC (34 mM)	119 ± 57	Spherical	High
TSC (50 mM)	81 ± 28	Spherical	High
HH	68 ± 24	Spherical	Moderate
AA	52 ± 9	Spherical	High

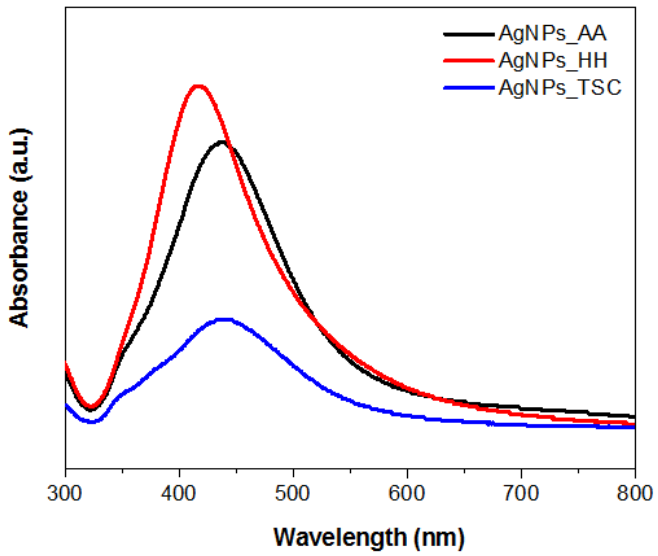

Figure 7.12. *Absorption spectra of AgNPs synthesized by using three different approaches.*

7.2. Preparation of AgNPs Decorated-Expanded Graphite Nanocomposite Powders

7.2.1. Production of Expanded Graphite (EG)

In this study, EG material with expansion ratio of 378 mL/g was prepared by rapid heating of expandable graphite at 1000°C for 2 min. Fig 7.13 shows the FEG-SEM images of expandable graphite and the EG prepared from it. As seen in Fig. 7.13 (b) and (c), layered structure of expandable graphite flake (Fig. 7.13 (a)) was transformed into a highly porous worm-like structure. This is a result of the decomposition of intercalating agent between the graphene layers when heating at high temperature and creating a pressure which separate the layers while still keeping them connected at some parts [56-58].

7.2.2. Decoration of EG with AgNPs synthesized using TSC as a reducing agent

AgNPs synthesized by using 34 mm TSC was used for decoration. Colloidal AgNPs (~90 ml) and EG (~0.5 g) powder were mixed together and EG was coated with AgNPs by using a rotary evaporator. SEM analysis were performed to evaluate the distribution of the AgNPs throught the EG particles (Fig. 7.14). These images reveal that AgNPs were uniformly coated onto the EG particles (on the surface of graphene layers, at the edges of these layers, into the pores and micro- and nano-cavities). Some agglomerates of AgNPs observed in these

micrographs can be advantageous for SERS analyses. Because nano-scale gaps known as hotspots that give rise to the local electromagnetic fields as well as enhancement of Raman signal are produced between junctions of adjacent two or multiple AgNPs [11, 13]. EDX analysis of these EG/AgNPs nanocomposite powders revealed C, Na and Ag elements (Fig.7.15). Na element was supposed to originate from TSC as in agreement with the literature [85]. A negative charge is formed on the surface of the AgNPs by achieving electrostatic stabilization with the negatively charged citrate ions ($C_6H_5O_7^{-3}$) that are adsorbed on or interact with the AgNPs.

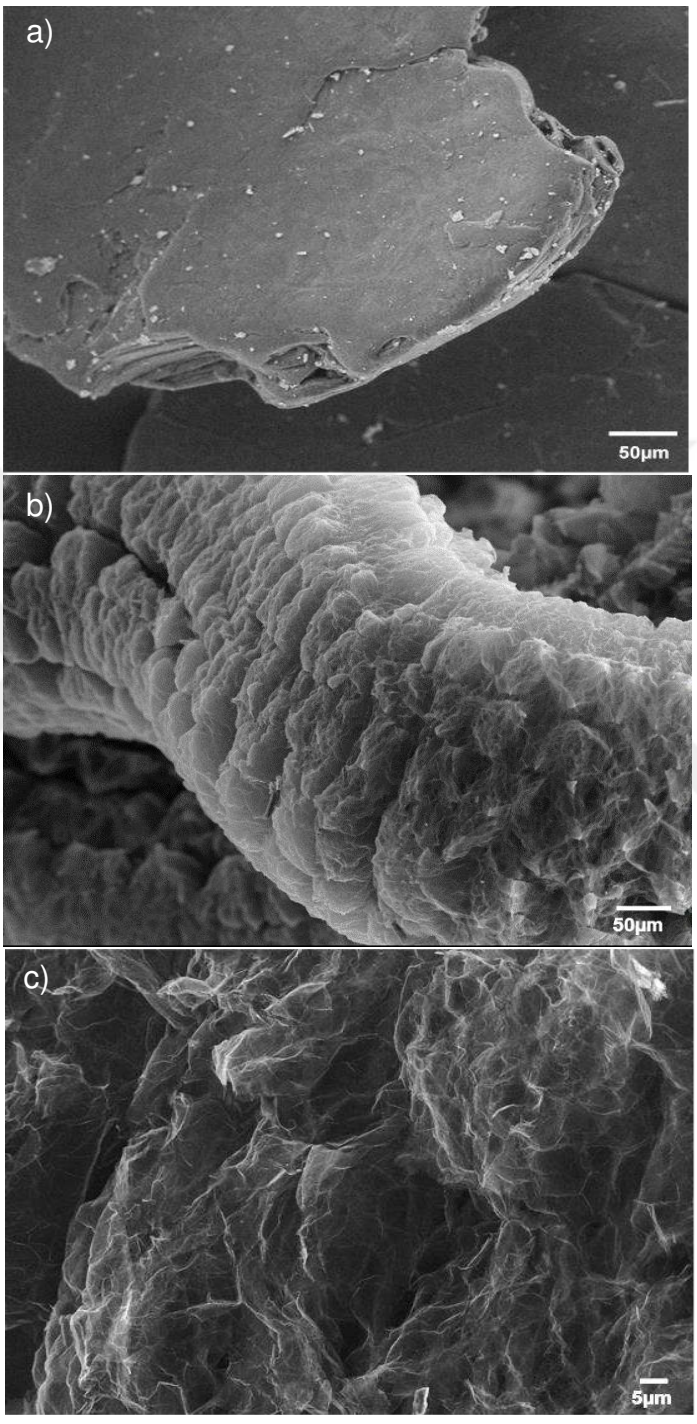

Figure 7.13. *FEG-SEM images of a) expandable graphite, EG b) at low magnification, c) at high magnification.*

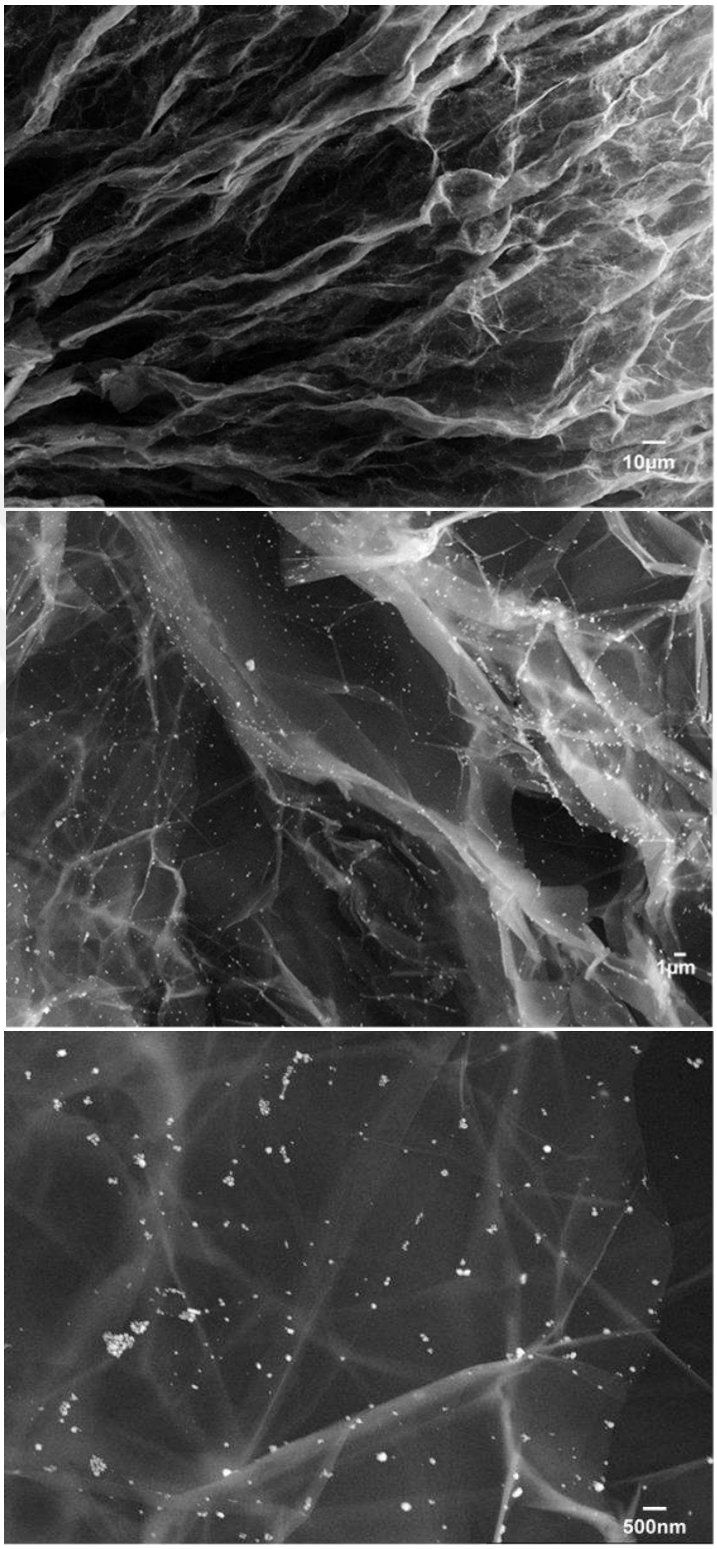

Figure 7.14. *FEG-SEM images of EG/AgNPs nanocomposite powders prepared by using 34mM TSC*.

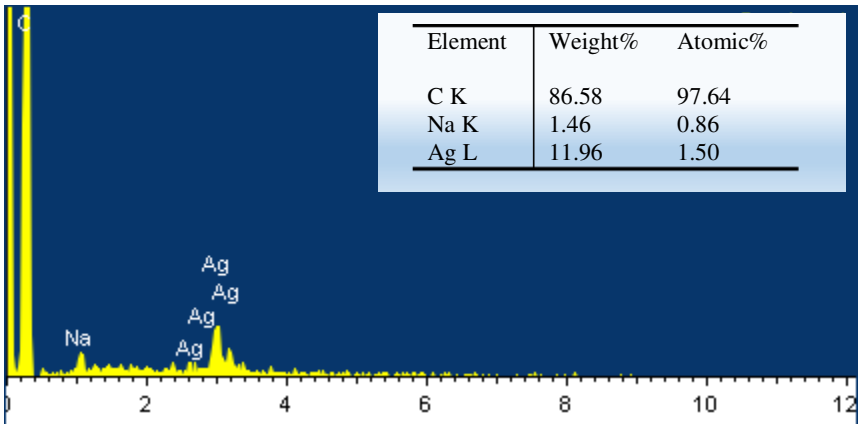

Figure 7.15. *EDX spectrum of EG/AgNPs nanocomposite powders prepared by using 34mM TSC.*

EG/AgNPs nanocomposite powder was also analyzed by XRD to investigate the present phases in this nanocomposite powder. Fig. 7.15 shows the XRD plot of this sample. The peaks observed at 2θ values of 26° and 54° are characteristic diffraction peaks of graphite ((002) and (004) planes, respectively) [56, 86]. Four diffraction peaks at 2θ = 38.1°, 44.3°, 64.4°, and 77.2° corresponds to the (111), (200), (220), and (311) crystalline planes of metallic silver, respectively. These results confirm that EG was decorated by AgNPs.

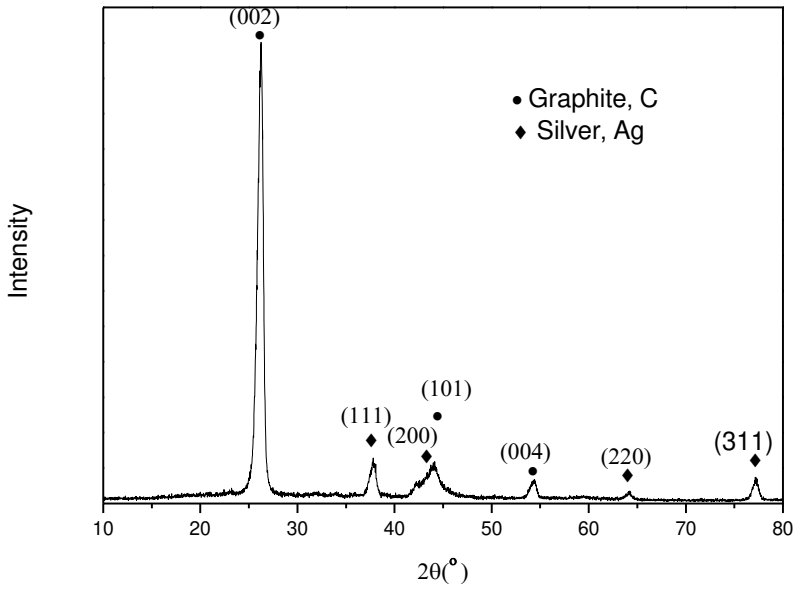

Figure 7.16. *XRD of EG/AgNPs nanocomposite powders prepared by using 34mM TSC.*

These characterization results confirmed that colloidal AgNPs were uniformly coated onto the EG particles in an easy way without requiring any complicated devices thanks to using rotary evaporator.

7.2.3. Decoration of EG with AgNPs synthesized using HH as a reducing agent

Figure 7.17 shows SEM images of EG/AgNPs nanocomposite powders prepared from AgNPs synthesized using HH as a reducing agent at different magnifications. It can be seen that AgNPs coated the surface of EG particle; however, the degree of agglomeration of AgNPs is much higher in comparison to the nanocomposite powder prepared from AgNPs synthesized using TSC. Although a certain amount of agglomeration of metallic nanoparticles is desired for SERS analysis, it could be detrimental for Raman signal enhancement if the amount of these agglomerates exceeds a certain amount [87]. The EDX analysis of this nanocomposite powder revealed C, Ag, Cl and O elements (Fig. 7.18). The detection of Cl was attributed to the chloride ions remaining from the synthesis of AgNPs that originate from HH and absorb on the surface of nanoparticles [81]. The presence of oxygen may indicate that some of the AgNPs were oxidized.

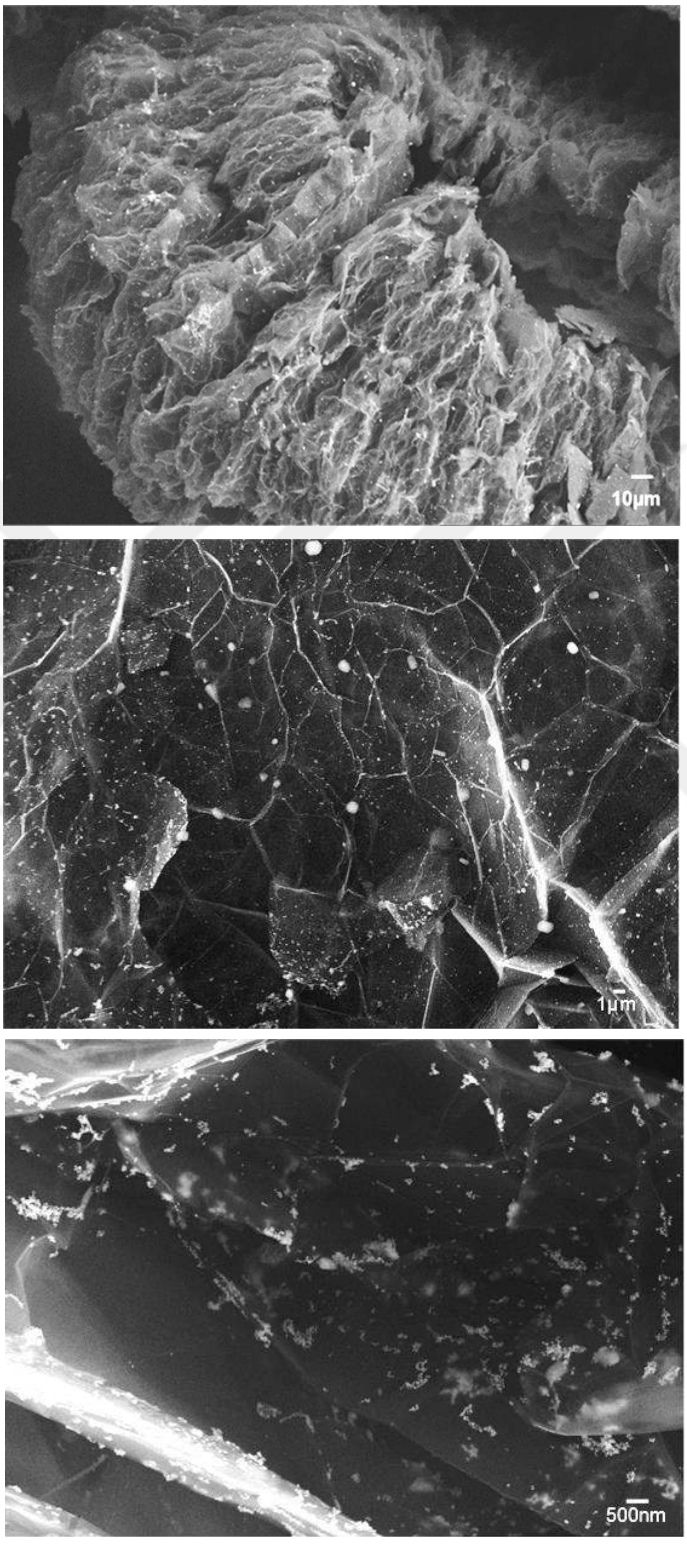

Figure 7.17. *FEG-SEM images of EG/AgNPs nanocomposite powders prepared by using HH.*

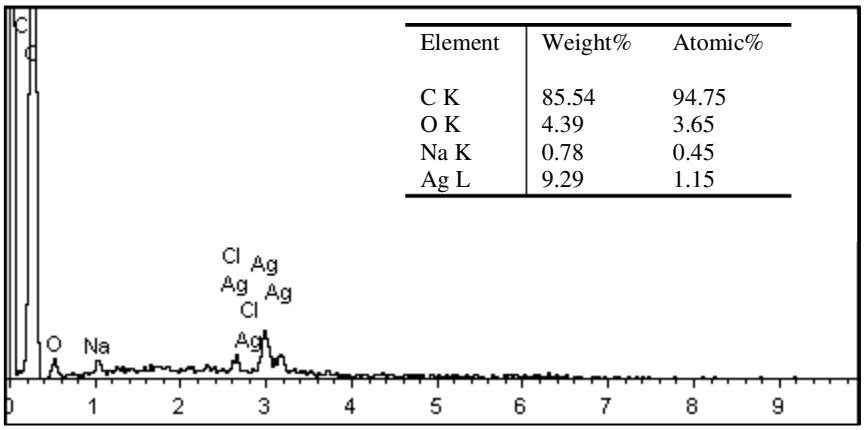

Element	Weight%	Atomic%
C K	85.54	94.75
O K	4.39	3.65
Na K	0.78	0.45
Ag L	9.29	1.15

Figure 7.18. *EDX spectrum of EG/AgNPs nanocomposite powders prepared by using HH.*

XRD pattern of EG/AgNPs nanocomposite powder prepared from AgNPs synthesized using HH is shown in Fig.7.19. The EG exhibited characteristic diffraction peaks of graphite at 2θ=26.4º and 54.4º which corresponded to the (002) and (004) crystal planes, respectively. The narrow and sharp peak of EG indicates its high degree of crystallinity. As it can be seen, crystal structure of graphite was not changed after rotary evaporation. The XRD analysis demonstrates the presence of AgNPs in the sample. It shows major diffraction peaks of metallic silver (fcc) at 2θ values of 38º, 44º, 64.3º and 77.3º, corresponding to (111), (200), (220) and (311) crystal planes, respectively. Peaks from halite phase (NaCl) were also observed. These peaks could be attributed to formation of NaCl crystals from sodium (Na^+) and chloride ions (Cl^-) during AgNPs synthesis.

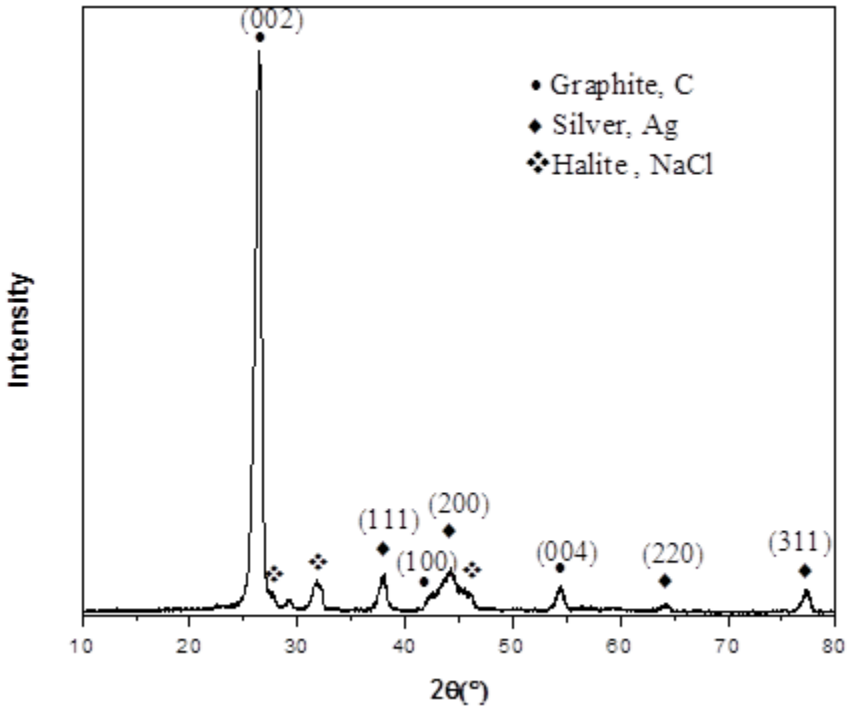

Figure 7.19. *XRD pattern of EG/AgNPs nanocomposite powders prepared by using HH.*

7.2.4. Decoration of EG with AgNPs synthesized using AA as a reducing agent

In Figure 7.20, the FEG-SEM image reveals that EG was decorated by AgNPs. Higher magnification image reveals some agglomerates of AgNPs which could be advantageous for SERS analyses.

The structure of sample was further confirmed by using XRD analysis as shown in Fig.7.22. A sharp (002) characteristic peak of graphite appeared at 2θ=26.3º and other diffraction peaks at 2θ values of 37.7º, 44º, 64º, 77.4º are indicated the presence of AgNPs. The absence of other phases in the XRD spectrum indicates that the product does not contain impurities.

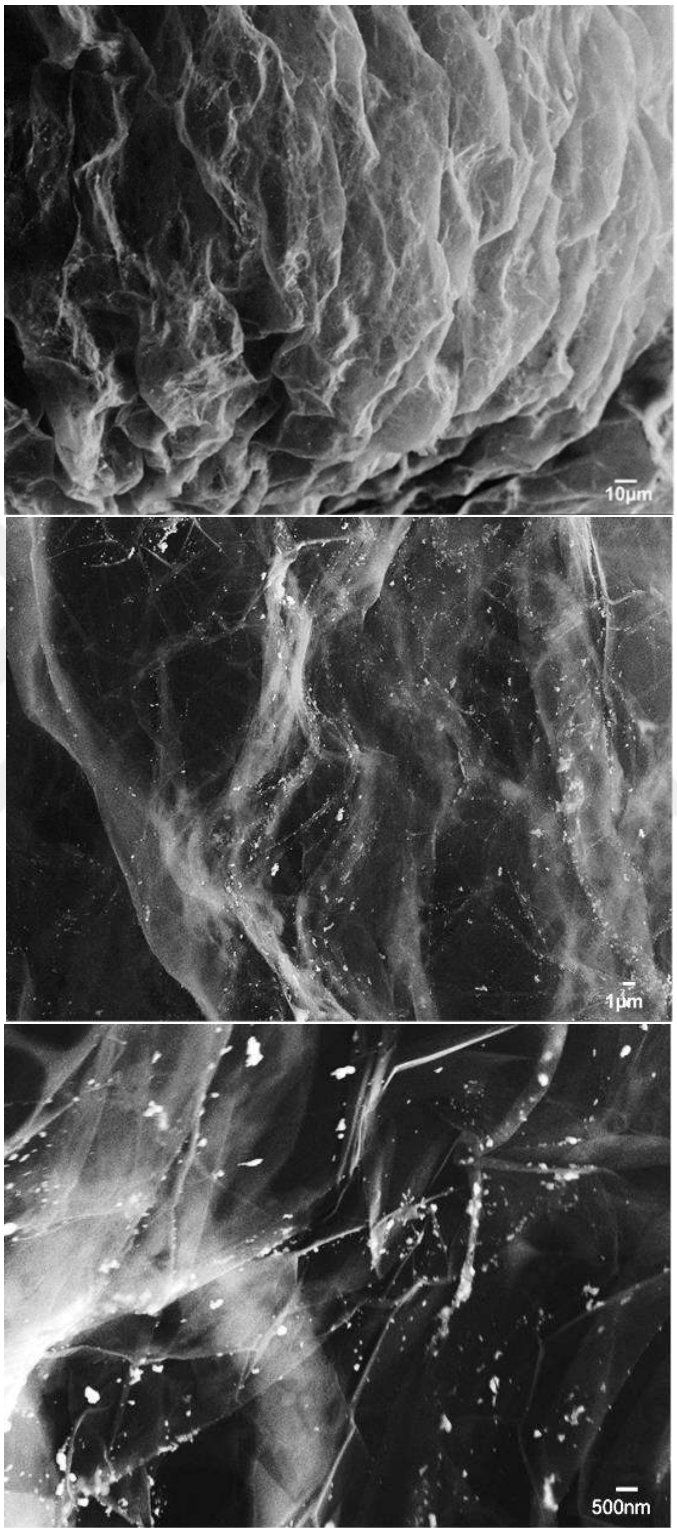

Figure 7.20. *FEG-SEM images of EG/AgNPs nanocomposite powders prepared by using AA.*

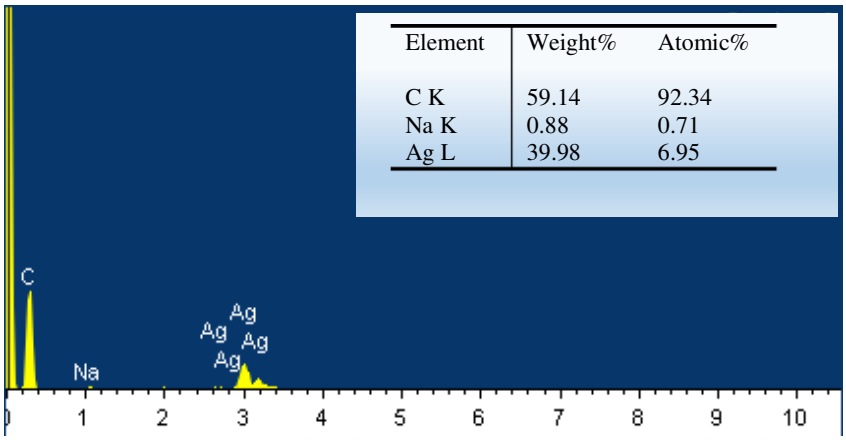

Figure 7.21. EDX spectrum of EG/AgNPs nanocomposite powders prepared by using AA.

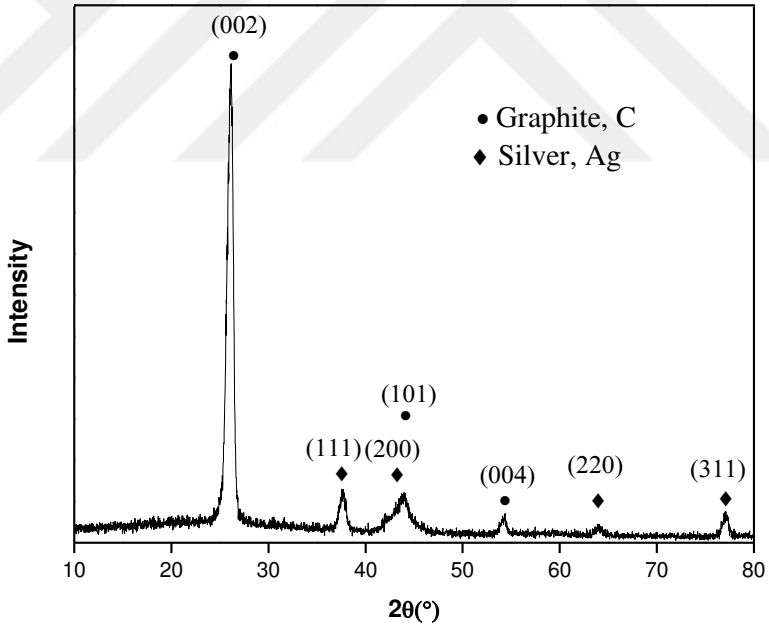

Figure 7.22. *XRD pattern of EG/AgNPs nanocomposite powders prepared by using AA.*

7.3. SERS Measurements

EG/AgNPs nanocomposites powders were compacted into the form of pellets to serve as 3D porous platforms for SERS analysis (Fig. 7.23).

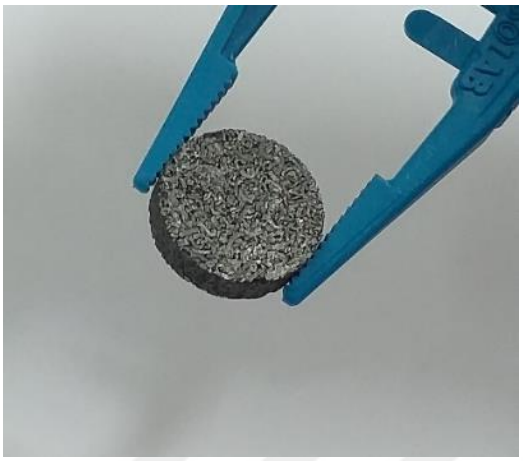

Figure 7.23. *The image of 3D porous EG/AgNPs pellet.*

SERS activity of the prepared substrates were tested using Rhodamine 6G as a standard analyte. R6G is a synthetic fluorescent dye which is widely used in acrylic, nylon, silk and wool dyeing, and it is critical to remove this dye from industrial waste-waters to protect human, environment and aquatic life [87]. SERS technique has an important role on detecting this molecule. Figure 7.24 shows the structure of R6G molecule. This molecule has two amine (NH) groups with which it can bind to AgNPs and expanded graphite [88].

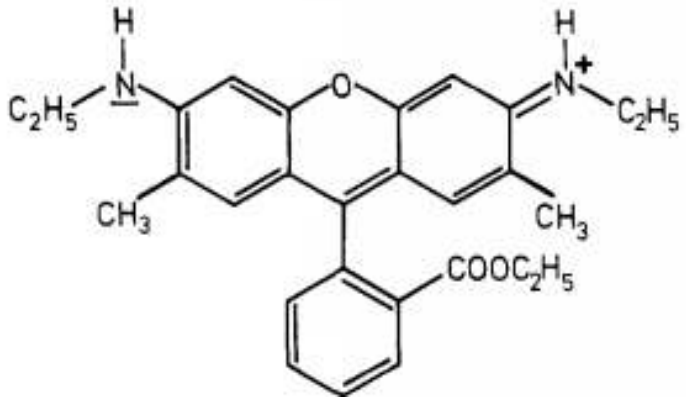

Figure 7.24. *Structural formula of R6G [89].*

R6G aqueous solutions with different concentrations (10^{-3} to 10^{-12} M) were prepared by serial dilution technique. SERS measurements were performed by drop-casting of 20 µL of analyte solution onto the substrate. Due to three dimensional porous structure of the substrates, the drop was absorbed within 1-3 min and the corresponding Raman spectra could immediately be recorded. Figure 7.25 shows the Raman spectra of R6G with different concentrations (10^{-3} to 10^{-7} M) on EG substrates. The detection limit of the EG substrates has been determined as 10^{-7} M. The corresponding Raman spectra revealed characteristic peaks of R6G molecule including 612 cm^{-1} and 771 cm^{-1} arising from out-of plane bending of C-H and C-C-C ring, respectively, 1182 and 1313 cm^{-1} due to in-plane bending of C-H and C-O-C stretchings, respectively, and 1364, 1511, 1580 and 1650 cm-1 arising from the C-C stretching of the aromatic ring [89, 90]. The SERS performance of these 3D porous EG platforms are similar to those reported by Sykam *et al.* [64] for their 2D flexible graphite sheet prepared from EG. It should be also noted that the EG that they produced is rather like a composite which contains a high amount of NaCl crystals on EG surface originating from the production process [64].

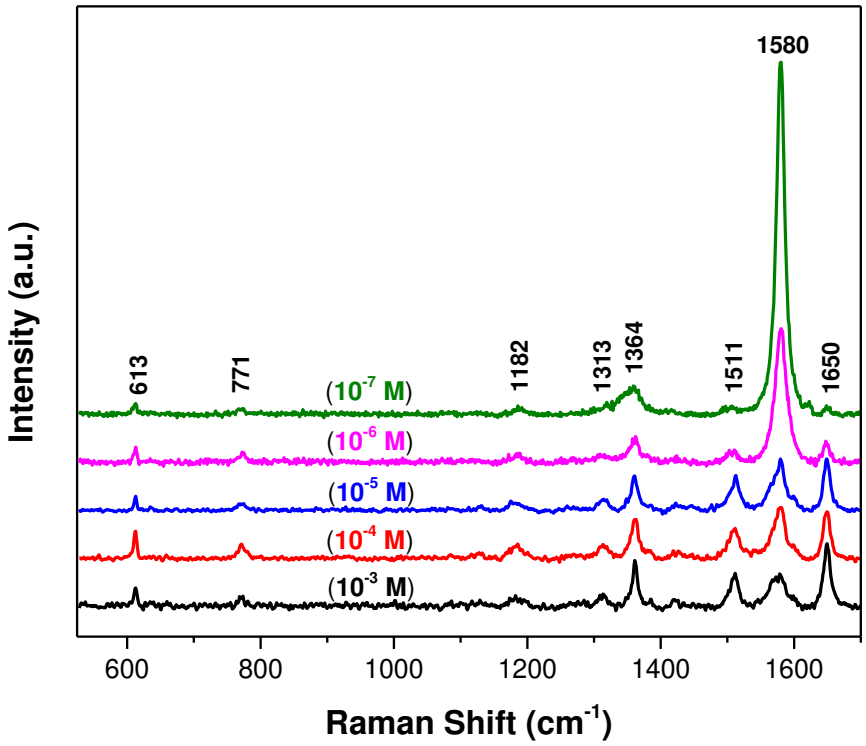

Figure 7.25. *Raman spectra of R6G with concentrations of 10^{-3} to 10^{-7} M on EG substrates.*

Raman spectra of R6G with different concentrations (10^{-3} to 10^{-8} M) were also recorded on EG substrates decorated with AgNPs produced by HH as a reducing agent (EG-AgNPs_HH). (Fig.7.26). Although the peaks of R6G were intensified when using AgNPs synthesized by HH route, the detection limit was still 10^{-7} M. This was attributed to polydisperse nature of these AgNPs and the presence of high amount of large agglomerates, which affect hot-spot formation negatively. It has been reported that the different sized agglomerates and the spacing between these agglomerates changes the SPR leading to variation in SERS signals [91].

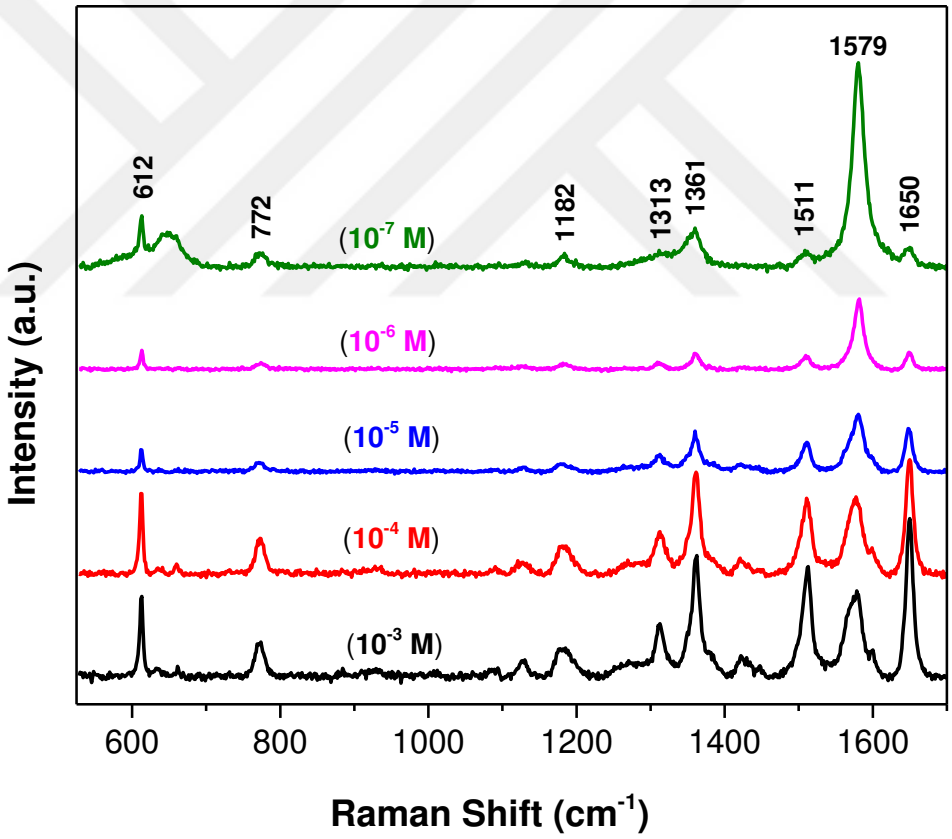

Figure 7.26. *Raman spectra of R6G (with concentrations of 10^{-3} to 10^{-7} M) on EG substrates decorated with AgNPs synthesized using hydroxylamine hydrochloride (HH) as a reducing agent (EG-AgNPs_HH).*

The detection limit of R6G molecules was successfully lowered to 10^{-11} M when substrates were prepared from EG decorated with AgNPs which were synthesized using AA

as a reducing agent (Fig.7.27). This result reveals high SERS sensitivity of the substrate. The monodispersed nature of these AgNPs with a relatively low average particle size (52 ±9 nm) and their uniform distribution throughout porous EG platform is thought to be effective in the enhancement of the Raman signals. Although Sykam *et al.* [64] reported that they could detect 10^{-12} M R6G using their 2D flexible graphite sheets as SERS substrates, they did not present these results in detail in their manuscript and they did not give much information about how they prepared their AgNPs decorated EG samples. The only reference that they orient the reader about AgNPs deposition process on EG [92] includes a complicated method. However, in this thesis study the EG powder was decorated by AgNPs easily, fastly and in a relatively low cost way by using a rotary evaporator.

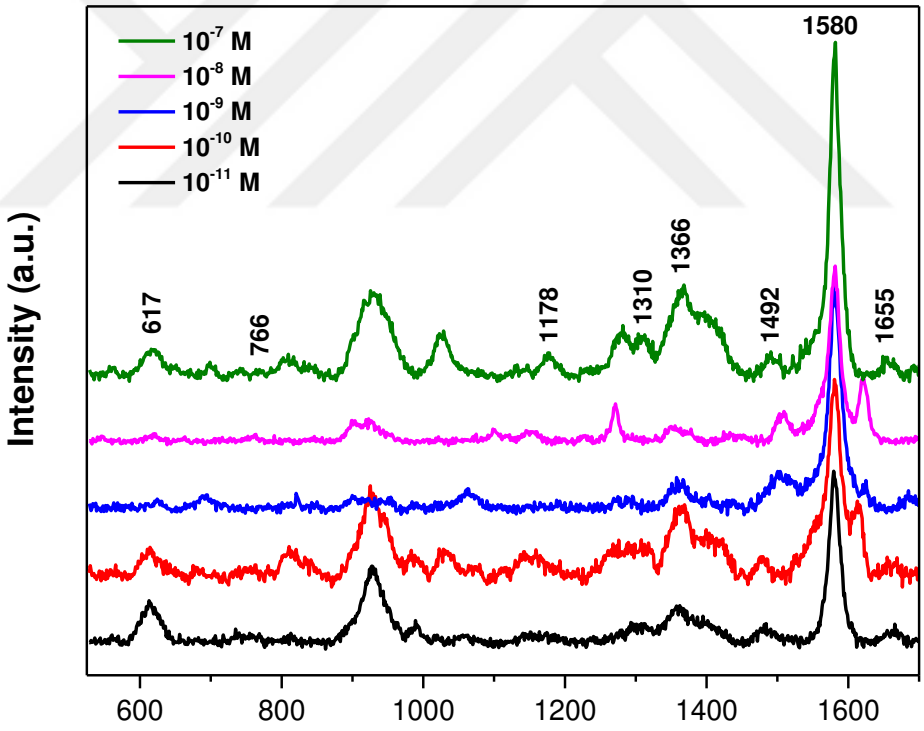

Figure 7.27. *Raman spectra of R6G (with concentrations of 10^{-7} to 10^{-11} M) on EG substrates decorated with AgNPs synthesized using ascorbic acid (AA) as a reducing agent (EG-AgNPs_AA).*

In Fig.7.28, the SERS performance of the EG and the AgNPs-decorated EG substrates on detection of 10^{-6} M R6G was compared. It can be clearly seen that three-dimensional porous EG substrate could detect 10^{-6} M R6G; however, the characteristic peaks of R6G was

intensified when this material was decorated with AgNPs. This intensification is especially much stronger when EG was decorated with AgNPs which were synthesized using AA as a reducing agent rather than HH.

Raman spectra of 10^{-4} M R6G recorded from 9 randomly selected spots on a EG-AgNPs_AA substrate exhibit a similar profile with slight deviations in the intensity of the characteristic Raman peaks of R6G, revealing the uniformity of this substrate (Fig.7.29).

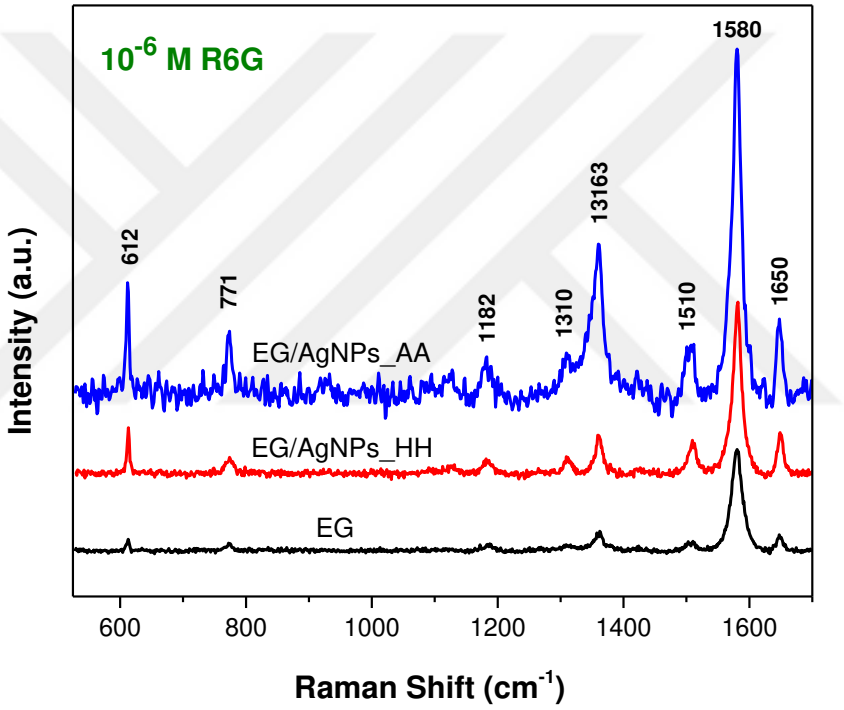

Figure 7.28. *Raman spectra of 10^{-6} M R6G on EG, EG-AgNPs_HH and EG-AgNPs_AA substrates.*

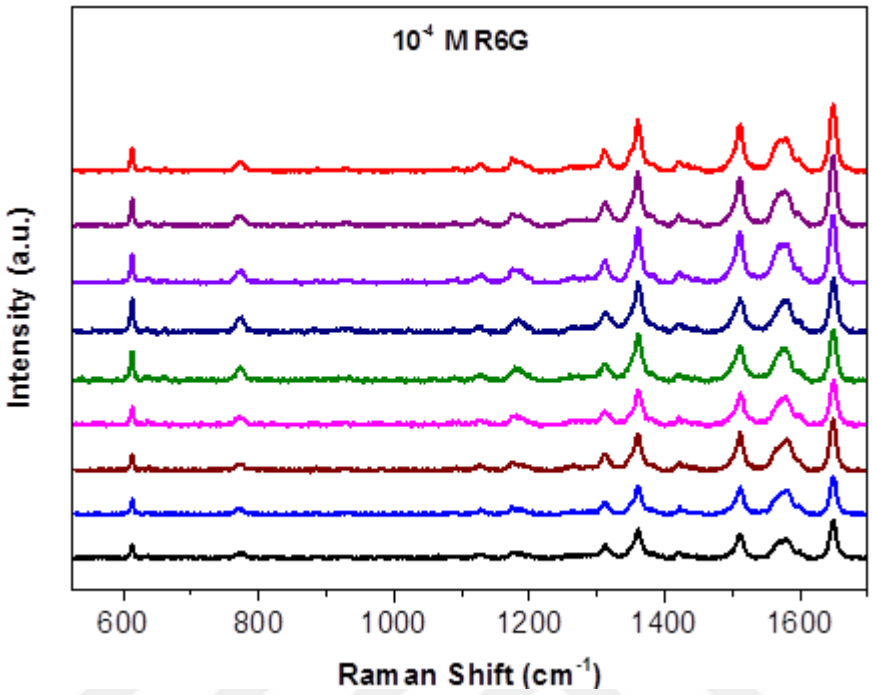

Figure 7.29. *Raman spectra of 10^{-4} M R6G that were recorded from 9 randomly selected spots on a EG_AgNPs_AA substrate.*

8. CONCLUSIONS

In this thesis, it was aimed to develop 3D porous platforms for rapid and routine SERS analyses in a low cost. For this purpose, SERS platforms were prepared from AgNPs decorated-expanded graphite while preserving the porous nature of the expanded graphite material. So that, it was utilized from the electromagnetic enhancement effect of AgNPs and chemical enhancement effect of graphene-based materials on Raman signals, and from the advantages of porous materials. Porous nature of these platforms enabled fast penetration of solvent into the platform providing fast Raman measurements and uniform distribution of AgNPs and analyte molecules. Accordingly, low detection limits (down to 10^{-11} M) of R6G dye molecules could be obtained by using these paltforms as SERS substrates.

The key results of this thesis study are summarized below:

- EG materials with an expansion ratio of 378 mg/l were prepared; AgNPs were successfully synthesized; and AgNPs were successfully coated on EG by rotary evaporator.
- The corresponding Raman spectra could be immediately recorded due to 3D porous nature of the substrates.
- The 3D porous EG platforms without any AgNPs decoration could detect 10^{-7} M R6G dye.
- The characteristic peaks of R6G was intensified when 3D porous EG platforms were decorated with AgNPs.
- The detection limit of R6G molecules was successfully reduced to 10^{-11} M when EG was decorated with AgNPs synthesized using ascorbic acid as a reducing agent.
- 3D porous EG platforms decorated with AgNPs were prepared in a low cost without using any sophisticated equipments and their potential as a highly efficient SERS substrate was revealed.

9. FUTURE PLAN

- SERS measurements of 3D porous EG platforms decorated with AgNPs synthesized by TSC will be performed.
- SERS measurements will be repeated by preparing R6G solutions in ethanol.
- EG will be functionalized and its effect on SERS performance will be investigated.
- Enhancement factors will be calculated.

REFERENCES

[1] Ewen, S., and Geoffrey, D. (2005). Modern Raman spectroscopy: a practical approach. New York: John Wiler & Sons.

[2] Larkin, P. (2017). Infrared and Raman spectroscopy: principles and spectral interpretation. Elsevier.

[3] Farcau, C., and Astilean, S. (2014). Periodically nanostructured substrates for surface enhanced Raman spectroscopy. *Journal of Molecular Structure*, 1073, 102-111.

[4] Zoubir, A. (2012). Raman imaging: techniques and applications (vol. 168). Springer.

[5] Mikla, V. I., and Mikla, V. V. (2013). Medical imaging technology. Elsevier.

[6] Raman spectroscopy explained booklet, www.renishaw.com/en/raman spectroscopy-explained-25801. (deadline accessed date: 20.09.2018)

[7] Lewis, I. R., and Edwards, H. (2001). Handbook of Raman spectroscopy: from the research laboratory to the process line. CRC Press.

[8] B&W Tek, Inc., Raman Knowledge: An Introduction to Raman Spectroscopy, https://www.azom.com/article.aspx?ArticleID=13372. (deadline accessed date: 24.08.2017).

[9] Lou, X. T., Zhao, X. R., Lin, X., Zhang, M. L., Xu, L. J., Wang, H. R., Hasi, W. L. J., Lu, Z. W. (2017). A simple drop-and-detect method using porous alumina ceramics as platforms for rapid surface-enhanced Raman spectroscopy *Journal of Raman Spectroscopy*, 48 (1): 89-96.

[10] Guo, H., He, L., and Xing, B. (2017). Applications of surface-enhanced Raman spectroscopy in the analysis of nanoparticles in the environment. *Environmental Science: Nano*, 4 (11), 2093-2107.

[11] Petryayeva, E. and Krull, U. J. (2011). Localized surface plasmon resonance: Nanostructures, bioassays and biosensing-A review. *Analytica Chimica Acta*, 706 (1): 8-24.

[12] Fleischmann, M., Hendra P. J. and McQuillan, A. J. (1974). Raman spectra of pyridine adsorbed at a silver electrode. *Chemical Physics Letters*, 26 (2): 163-166.

[13] Maher, R. C. (2012). SERS Hot Spots. Raman Spectroscopy for Nanomaterials Characterization. C. S. S. R. Kumar. Berlin, Heidelberg, Springer Berlin Heidelberg: 215-260.

[14] Jeanmaire, D. L. ve Van Duyne, R. P. (1977). Surface raman spectroelectrochemistry. *Journal of Electroanalytical Chemistry and Interfacial Electrochemistry*, 84 (1): 1-20.

[15] Albrecht, M. G. ve Creighton, J. A. (1977). Anomalously intense Raman spectra of pyridine at a silver electrode. *Journal of the American Chemical Society*, 99 (15): 5215-5217.

[16] Moskovits, M. (1978). Surface roughness and the enhanced intensity of Raman scattering by molecules adsorbed on metals. *Journal of Chemical Physics*, 69 (9): 4159-4161.

[17] Nie, S. ve Emory S. R. (1997). Probing Single Molecules and Single Nanoparticles by Surface-Enhanced Raman Scattering. *Science*, 275 (5303): 1102-1106.

[18] Kneipp, K., Kneipp, H., Itzkan, I., Dasari, R. R., Feld, M. S. (1999). Surface-enhanced non-linear Raman scattering at the single-molecule level. *Chemical Physics*, 247 (1):155-162.

[19] Alarcon, E. I., Griffith, M., and Udekwu, K. I. (2015). *Silver nanoparticle applications.* New York: Springer.

[20] Sevenler, D., Ünlü, N. L., and Ünlü, M. S. (2015). Nanoparticle biosensing with interferometric reflectance imaging. In *Nanobiosensors and Nanobioanalyses* (pp. 81-95). Springer, Tokyo.

[21] Chang, H. W., Hsu, P. C., and Tsai, Y. C. (2012). Ag/carbon nanotubes for surface-enhanced Raman scattering. In *Raman spectroscopy for nanomaterials characterization* (pp. 119-135). Springer, Berlin, Heidelberg.

[22] Le Ru, E. C., Blackie, E., Meyer, M., and Etchegoin, P. G. (2007). Surface enhanced Raman scattering enhancement factors: a comprehensive study. *The Journal of Physical Chemistry C*, 111 (37), 13794-13803.

[23] Ouyang, L., Ren, W., Zhu, L. H., Irudayaraj J. (2017). Prosperity to challenges: recent approaches in SERS substrate fabrication. *Reviews in Analytical Chemistry*, 36 (1).

[24] Walsh, R. J. and Chumanov, G. (2001). Silver coated porous alumina as a new substrate for surface-enhanced Raman scattering. *Applied Spectroscopy*, 55 (12): 1695-1700.

[25] Gomez, M. and Lazzari, M. (2014). Reliable and cheap SERS active substrates Ordered vs disordered. *Materials Today*, 17 (7): 358-359.

[26] Sharma, B., Frontiera, R. R., Henry, A. I., Ringe, E., Van Duyne, R. P. (2012). SERS: Materials, applications, and the future. *Materials Today*, 15 (1-2): 16-25.

[27] Zhang, X. F., Liu, Z. G., Shen, W., Gurunathan, S. (2016). Silver nanoparticles: synthesis, characterization, properties, applications, and therapeutic approaches. *International journal of molecular sciences*, 17 (9), 1534.

[28] El-Badawy, A., Feldhake, D., and Venkatapathy, R. (2010). State of the science literature review: everything nanosilver and more. *US Environmental Protection Agency*.

[29] Klabunde, K. J., and Richards, R. M. (Eds.). (2009). Nanoscale materials in chemistry. John Wiley & Sons.

[30] Dastafkan, K., Khajeh, M., Bohlooli, M., Ghaffari-Moghaddam, M., Sheibani, N. (2015). Mechanism and behavior of silver nanoparticles in aqueous medium as adsorbent. *Talanta*, 144, 1377-1386.

[31] Chouhan, N. (2018). Silver Nanoparticles: Synthesis, Characterization and Applications. K. Maaz (Ed.), inside of *Silver Nanoparticles-Fabrication, Characterization and Applications* (21-59). London: IntechOpen.

[32] LaMer, V. K. and Dinegar, R. H. (1950). Theory, production and mechanism of formation of monodispersed hydrosols. *Journal of the American Chemical Society*, 72 (11), 4847-4854.

[33] Cao, G., and Wang, Y., (2011). *Nanostructures and nanomaterials: synthesis, properties and applications.* (2nd edition). New Jersey: World Scientific.

[34] Turkevich, J., Stevenson, P. C., and Hillier, J. (1951). A study of the nucleation and growth processes in the synthesis of colloidal gold. *Discussions of the Faraday Society*, 11, 55-75.

[35] Lee, P. C., and Meisel, D. (1982). Adsorption and surface-enhanced Raman of dyes on silver and gold sols. *The Journal of Physical Chemistry*, 86 (17), 3391-3395.

[36] Wiley, B., Sun, Y., Mayers, B., Xia, Y. (2005). Shape-controlled synthesis of metal nanostructures: the case of silver. *Chemistry–A European Journal*, 11 (2), 454-463.

[37] Pillai, Z. S., and Kamat, P. V. (2004). What factors control the size and shape of silver nanoparticles in the citrate ion reduction method?. *The Journal of Physical Chemistry B*, 108 (3), 945-951.

[38] Choi, Y., Song, S. W., Hooch Antink, W., Kim, H. M., Piao, Y. (2017). A silver/graphene oxide nanocomposite film as a flexible SERS substrate for reliable quantitative analysis using high-speed spiral scanning spectrometry. *Chemical Communications.*

[39] Suzuki, S. and M. Yoshimura (2017). Chemical Stability of Graphene Coated Silver Substrates for Surface-Enhanced Raman Scattering. *Scientific Reports*, 7.

[40] Li, X., Lee, H. K., Phang, I. Y., Lee, C. K., Ling, X. Y. (2014). Superhydrophobic-Oleophobic Ag Nanowire Platform: An Analyte-Concentrating and Quantitative Aqueous and Organic Toxin Surface-Enhanced Raman Scattering Sensor. *Analytical Chemistry*, 86 (20): 10437-10444.

[41] Lee, J., Shin, S., Kang, S., Lee, S., Seo, J., Lee, T. (2015). Highly Stable Surface-Enhanced Raman Spectroscopy Substrates Using Few-Layer Graphene on Silver Nanoparticles. *Journal of Nanomaterials*.

[42] Hirakawa, T. and P. V. Kamat (2005). Charge separation and catalytic activity of Ag@TiO_2 core-shell composite clusters under UV-irradiation. *Journal of the American Chemical Society*, 127 (11): 3928-3934.

[43] Liz-Marzan, L. M., M. Giersig and P. Mulvaney (1996). Synthesis of nanosized gold-silica core-shell particles. *Langmuir*, 12 (18): 4329-4335.

[44] Ma, L., Huang, Y., Hou, M., Xie, Z., Zhang, Z. (2015). Silver nanorods wrapped with ultrathin Al_2O_3 layers exhibiting excellent SERS sensitivity and outstanding SERS stability. *Scientific reports*, *5*, 12890.

[45] Deschaines, T. O. and Wieboldt, D. (2010). Technical note 51874: Practical Applications of Surface Enchanced Raman Scattering (SERS), https://tools.thermofisher.com/content/sfs/brochures/D19663~.pdf. (deadline accessed date: 20.09.2018).

[46] Avci, E. ve Culha, M. (2013). Influence of droplet drying configuration on surface-enhanced Raman scattering performance. *Rsc Advances*, 3 (39): 17829-17836.

[47] Lee, A., Dubinsky, S., Tumarkin, E., Moulin, M., Beharry, A.A., Kumacheva, E. (2011). Multifunctional Hybrid Polymer-Based Porous Materials. *Advanced Functional Materials*, 21 (11): 1959-1969.

[48] Ji, N., Ruan, W. D., Wang, C. X., Lu, Z. C., Zhao, B. (2009). Fabrication of Silver Decorated Anodic Aluminum Oxide Substrate and Its Optical Properties on Surface-Enhanced Raman Scattering and Thin Film Interference. *Langmuir,* 25 (19): 11869-11873.

[49] Zeiri, L., Rechav, K., Porat, Z., Zeiri, Y. (2012). Silver Nanoparticles Deposited on Porous Silicon as a Surface-Enhanced Raman Scattering (SERS) Active Substrate. *Applied Spectroscopy*, 66 (3): 294-299.

[50] Pan, Z., Zavalin, A., Ueda, A., Guo, M., Groza, M., Burger, A., Mu, R., Morgan, S. H. (2005). Surface-enhanced Raman spectroscopy using silver-coated porous glass-ceramic substrates. *Applied Spectroscopy*, 59 (6): 782-786.

[51] Pack, M., Hu, H., Kim, D. O., Yang, X., Sun, Y. (2015). Colloidal Drop Deposition on Porous Substrates: Competition among Particle Motion, Evaporation, and Infiltration. *Langmuir*, 31 (29): 7953-7961.

[52] Xu, Y., Yang, C., Wang, M., Pan, X., Zhang, C., Liu, M., Xu, S., Jiang, S., Man, B. (2017). Adsorbable and self-supported 3D AgNPs/G@ Ni foam as cut-and-paste highly-sensitive SERS substrates for rapid in situ detection of residuum. *Optics express*, 25 (14), 16437-16451.

[53] Lu, R., Sha, J., Xia, W., Fang, Y., Gu, L., Wang, Y. (2013). A 3D-SERS substrate with high stability: Silicon nanowire arrays decorated by silver nanoparticles. *CrystEngComm,* 15 (31), 6207-6212.

[54] Vendamani, V. S., Nageswara Rao, S. V. S., Venugopal Rao, S., Kanjilal, D., Pathak, A. P. (2018). Three-dimensional hybrid silicon nanostructures for surface enhanced Raman spectroscopy based molecular detection. *Journal of Applied Physics*, 123 (1), 014301.

[55] Celzard, A., Mareche, J. F., and Furdin, G. (2005). Modelling of exfoliated graphite. *Progress in Materials Science*, 50 (1), 93-179.

[56] Celik, Yasemin. Production of graphene based materials and their potential applications. PhD Thesis, Joint Supervision of Thesis (Cotutelle) between Anadolu University and Université Toulouse III Paul Sabatier, 2015.

[57] https://asbury.com/resources/education/science-of-graphite. (deadline accessed date: 10.07.2019).

[58] Chung, D. D. L. (2016). A review of exfoliated graphite. *Journal of materials science*, *51* (1), 554-568.

[59] Liu, Y., and Yang, Y. (2018). Form-stable phase change material based on $Na_2CO_3 \cdot 10H_2O$-$Na_2HPO_4 \cdot 12H_2O$ eutectic hydrated salt/expanded graphite oxide composite: The influence of chemical structures of expanded graphite oxide. *Renewable energy*, 115, 734-740.

[60] Li, X. Y., Li, J., Zhou, X. M., Ma, Y. Y., Zheng, Z. P., Duan, X. F., Qu, Y. Q. (2014). Silver nanoparticles protected by monolayer graphene as a stabilized substrate for surface enhanced Raman spectroscopy. *Carbon*, 66: 713-719.

[61] Ling, X., Xie, L. M., Fang, Y., Xu, H., Zhang, H. L., Kong, J., Dresselhaus, M. S., Zhang, J., Liu, Z. F. (2010). Can Graphene be used as a Substrate for Raman Enhancement?. *Nano Letters*, 10 (2): 553-561.

[62] Kim, Y. K., Han, S. W. and Min, D. H. (2012). Graphene Oxide Sheath on Ag Nanoparticle/Graphene Hybrid Films as an Antioxidative Coating and Enhancer of Surface-Enhanced Raman Scattering. *Acs Applied Materials & Interfaces*, 4 (12): 6545-6551.

[63] Wang, X., Zhu, C., Huang, Z., Hu, X., Zhu, X. (2016). In situ synthesis of pristine-graphene/Ag nanocomposites as highly sensitive SERS substrates. *RSC Advances, 6* (94), 91579-91583.

[64] Sykam, N., Jayram, N. D., and Rao, G. M. (2019). Exfoliation of graphite as flexible SERS substrate with high dye adsorption capacity for Rhodamine 6G. *Applied Surface Science*, 471, 375-386.

[65] Leopold, N., Lendl, B. (2003). A new method for fast preparation of highly surface-enhanced Raman scattering (SERS) active silver colloids at room temperature by reduction of silver nitrate with hydroxylamine hydrochloride. *The Journal of Physical Chemistry B*, 107 (24), 5723-5727.

[66] Cheng, Z. P., Chu, X. Z., Wu, X. Q., Xu, J. M., Zhong, H., Yin, J. Z. (2017). Controlled synthesis of silver nanoplates and nanoparticles by reducing silver nitrate with hydroxylamine hydrochloride. *Rare Metals*, 36 (10), 799-805.

[67] Ciftci, H., Türk K, M., Tamer, U., Karahan, S., & Menemen, Y. (2013). Silver nanoparticles: cytotoxic, apoptotic, and necrotic effects on MCF-7 cells. *Turkish Journal of Biology*, 37 (5), 573-581.

[68] Qin, Y., Ji, X., Jing, J., Liu, H., Wu, H., Yang, W. (2010). Size control over spherical silver nanoparticles by ascorbic acid reduction. *Colloids and Surfaces A: Physicochemical and Engineering Aspects,* 372 (1-3), 172-176.

[69] Mendis, P., de Silva, R. M., de Silva, K. N., Wijenayaka, L. A., Jayawardana, K., Yan, M. (2016). Nanosilver rainbow: a rapid and facile method to tune different colours of nanosilver through the controlled synthesis of stable spherical silver nanoparticles. *RSC Advances*, 6 (54), 48792-48799.

[70] Gong, T., Zhu, Y., Zhang, J., Ren, W., Quan, J., Wang, N. (2015). Study on surface-enhanced Raman scattering substrates structured with hybrid Ag nanoparticles and few-layer graphene. *Carbon*, 87, 385-394.

[71] Meng, W., Hu, F., Jiang, X., and Lu, L. (2015). Preparation of silver colloids with improved uniformity and stable surface-enhanced Raman scattering. *Nanoscale research letters*, *10* (1), 34.

[72] Hu, M., Chen, J., Li, Z. Y., Au, L., Hartland, G. V., Li, X., Marquez, M., Xia, Y. (2006). Gold nanostructures: engineering their plasmonic properties for biomedical applications. *Chemical Society Reviews*, 35 (11), 1084-1094.

[73] Shang, J. and Gao, X. (2014). Nanoparticle counting: towards accurate determination of the molar concentration. *Chemical Society Reviews*, 43 (21), 7267-7278.

[74] Ranoszek-Soliwoda, K., Tomaszewska, E., Socha, E., Krzyczmonik, P., Ignaczak, A., Orlowski, P., Krzyzowska, M., Celichowski, G., Grobelny, J. (2017). The role of tannic acid and sodium citrate in the synthesis of silver nanoparticles. *Journal of Nanoparticle Research*, 19 (8), 273.

[75] Lee, S. H., and Jun, B. H. (2019). Silver Nanoparticles: Synthesis and application for nanomedicine. *International journal of molecular sciences*, 20 (4), 865.

[76] Henglein, A., and Giersig, M. (1999). Formation of colloidal silver nanoparticles: capping action of citrate. *The Journal of Physical Chemistry B*, 103 (44), 9533-9539.

[77] Krutyakov, Y. A., Kudrinskiy, A. A., Olenin, A. Y., Lisichkin, G. V. (2008). Synthesis and properties of silver nanoparticles: advances and prospects. *Russian Chemical Reviews*, 77 (3), 233.

[78] Mondal, B., and Saha, S. K. (2010). Fabrication of SERS substrate using nanoporous anodic alumina template decorated by silver nanoparticles. *Chemical Physics Letters*, *497* (1-3), 89-93.

[79] Stamplecoskie, K. G., Scaiano, J. C., Tiwari, V. S., Anis, H. (2011). Optimal size of silver nanoparticles for surface-enhanced Raman spectroscopy. *The Journal of Physical Chemistry C*, *115* (5), 1403-1409.

[80] Canamares, M. V., Garcia-Ramos, J. V., Gomez-Varga, J. D., Domingo, C., Sanchez-Cortes, S. (2005). Comparative study of the morphology, aggregation, adherence to glass, and surface-enhanced Raman scattering activity of silver nanoparticles prepared by chemical reduction of Ag^+ using citrate and hydroxylamine. *Langmuir*, 21 (18), 8546-8553.

[81] Garrido, C., Weiss-Lopez, B. E., and Campos Vallette, M. M. (2016). Surface-enhanced Raman scattering activity of negatively charged bio-analytes from a modified silver colloid. *Spectroscopy Letters*, 49 (1), 11-18.

[82] Li, H., Xia, H., Wang, D., and Tao, X. (2013). Simple synthesis of monodisperse, quasi-spherical, citrate-stabilized silver nanocrystals in water. *Langmuir*, 29(16), 5074-5079.

[83] Alqadi, M., Noqtah, O. A., Alzoubi, F., Alzouby, J., Aljarrah, K. (2014). pH effect on the aggregation of silver nanoparticles synthesized by chemical reduction. *Materials Science-Poland*, 32 (1), 107-111.

[84] LaMer, V. K., and Dinegar, R. H. (1950). Theory, production and mechanism of formation of monodispersed hydrosols. *Journal of the American Chemical Society*, 72 (11), 4847-4854.

[85] Ding, G., Xie, S., Liu, Y., Wang, L., Xu, F. (2015). Graphene oxide-silver nanocomposite as SERS substrate for dye detection: Effects of silver loading amount and composite dosage. *Applied Surface Science*, 345, 310-318.

[86] Hou, S., Li, J., Huang, X., Wang, X., Ma, L., Shen, W., Kang, F., Huang, Z. H. (2017). Silver Nanoparticles-Loaded Exfoliated Graphite and Its Anti-Bacterial Performance. *Applied Sciences*, 7 (8), 852.

[87] Vanamudan, A., and Pamidimukkala, P. (2015). Chitosan, nanoclay and chitosan–nanoclay composite as adsorbents for Rhodamine-6G and the resulting optical properties. *International journal of biological macromolecules*, 74, 127-135.

[88] Kalele, S., Deshpande, A. C., Singh, S. B., Kulkarni, S. K. (2008). Tuning luminescence intensity of RHO6G dye using silver nanoparticles. *Bulletin of Materials Science*, 31 (3), 541-544.

[89] Hildebrandt, P., and Stockburger, M. (1984). Surface-enhanced resonance Raman spectroscopy of Rhodamine 6G adsorbed on colloidal silver. *The Journal of Physical Chemistry*, 88 (24), 5935-5944.

[90] Huang, D., Cui, J., and Chen, X. (2014). A morpholinium surfactant crystallization induced formation of Au nanoparticle sheet-like assemblies with uniform SERS activity. *Colloids and Surfaces A: Physicochemical and Engineering Aspects*, 456, 100-107.

[91] Yaffe, N. R., Ingram, A., Graham, D., Blanch, E. W. (2010). A multi-component optimization of experimental parameters for maximizing SERS enhancements. *Journal of Raman spectroscopy*, 41 (6), 618-623.

[92] Jayram, N. D., Sonia, S., Kumar, P. S., Marimuthu, L., Masuda, Y., Mangalaraj, D., Ponpandian, N., Viswanathan, C., Ramakrishna, S. (2015). Highly monodispersed Ag embedded SiO_2 nanostructured thin film for sensitive SERS substrate: growth, characterization and detection of dye molecules. *RSC Advances*, 5 (57), 46229-46239.

.

RESUME

Name Surname : Ayse Kurt

Foreign Language: English

Place and Date of Birth : Eskisehir/ 15.08.1982

E-mail : aysekurt@eskisehir.edu.tr, kurtayse@gmail.com

Education and Professional Background:

- 2012-2014, Researcher, BAP Project (1204F070) titled "Preparation and Characterization of Cellulose Based Biodegradable Nanocomposites", Anadolu University
- 2005, Anadolu University, Bachelor in Materials Science and Engineering

Publications and / or Scientific / Artistic Activities:

- 2018, oral presentation, IV. International Ceramics, Glass, Enamel, Glaze and Paint Congress (SERES'18), Production of expanded graphite with a controlled pore structure as a carbon support material, Eskisehir, Turkey.
- Çelebi H, Kurt A. (2015). Effects of processing on the properties of chitosan/cellulose nanocrystal films. Carbohydrate Polymers, 133, 284-293.
- 2014, oral presentation, 16th European Conference for Composite Materials (ECCM16), Thermal and Mechanical Properties of PLA /PEG Blend and its Nanocomposites, Seville, Spain.
- 2013, poster presentation, Frontiers in Polymer Science, Structure and thermal properties of the chitosan/cellulose whisker nanocomposite films, Barcelona, Spain.
- 2013, poster presentation, International Porous and Powder Materials Symposium and Exhibition (PPM2013), Cellulose Nanowhisker/ PLA Composites: Processing and Characterization, International Porous and Powder Materials Symposium and Exhibition, Izmir, Turkey.
- 2012, poster presentation, 4th National Polymer Science and Technology Congress. Preparation of Cellulose Nanowhisker Based Polymer Nanocomposites and Development of Mechanical-Thermal Properties, Canakkale, Turkey.